A GIS INVESTIGATION OF PAIRED WATERSHEDS: ICEHOUSE CANYON AND UPPER SAN ANTONIO CANYON, EASTERN SAN GABRIEL MOUNTAINS

A Thesis

Presented to the

Faculty of

California State Polytechnic University, Pomona

In Partial Fulfillment

Of the Requirements for the Degree

Master of Science

In

Geological Sciences

By

Susan L. Perez

2015

SIGNATURE PAGE

THESIS: A GIS INVESTIGATION OF PAIRED WATERSHEDS: ICEHOUSE CANYON AND UPPER SAN ANTONIO CANYON, EASTERN SAN GABRIEL MOUNTAINS

AUTHOR: Susan L. Perez

DATE SUBMITTED: Winter 2015

Geological Sciences Department

Dr. Jonathan A. Nourse
Thesis Committee Chair
Geological Sciences

[redacted] 3/20/15

Dr. Stephen G. Osborn
Geological Sciences

[redacted]

Dr. Jascha Polet
Geological Sciences

[redacted]

Dr. Nick Van Buer
Geological Sciences

[redacted]

ACKNOWLEDGEMENTS

I would like to thank the faculty, both current and emeritus, of California State Polytechnic University for all their patience, support, and mentorship during my undergraduate and graduate careers. Without them, this thesis would not have been possible. But I would like to especially thank Dr. Jon Nourse, my advisor; you have been the best teacher and friend and I so greatly appreciate it. I only wish I could spend more time with you learning geology, a subject that we love.

Thanks go to the three men in my life, Raul, Alexander, and Lorenzo for their love and support during this effort. I needed the help with dinners, thesis formatting issues, and the IT help using ArcMap when it seemed like all data was lost. And a final thank you to Mom and Dad; I miss you and wish you both were here to see this thesis.

ABSTRACT

Two paired watersheds, Upper San Antonio and Icehouse Canyons, located in the eastern San Gabriel Mountains were studied using a geographical information system (GIS) to examine the effects of rock and soil present, vegetation, hill shade, slope, aspect, and solar insolation variables on the baseflow recession rates.

Baseflow recession is the response of a watershed to influxes of precipitation during dry conditions. Baseflow recession constants for Icehouse and San Antonio Canyons were previously determined to be 0.0080 $days^{-1}$ and 0.0185 $days^{-1}$ respectively. Other researchers have speculated as to the causes of this difference and it is thought that the differences are partially due to the effects of vegetation, hill shade, differences in rock /soil types and amounts, and solar insolation on the baseflow recessions observed in the watersheds. An analysis of three different geological maps of the area and four map variables was conducted to determine their effects on baseflow recessions. Significant differences can be seen in the types and amounts of vegetation, the configuration of rock and soils present, the aspect for each canyon, and the amounts of solar insolation received by each canyon throughout the year. Aspect, hill shade, and solar insolation amounts all have an effect on the overall availability of water for plant use and is reflected in the types and locations of various plants seen in the study area. Colluvium, landslides, slope, and covered bedrock also play an important role in the availability of water either for storage and use by the vegetation or groundwater flow.

TABLE OF CONTENTS

LIST OF TABLES

LIST OF FIGURES

CHAPTER 1

INTRODUCTION

Paired watersheds have a distinct advantage in that comparisons can be made of various environmental controls that directly affect the water budget of both watersheds, as well as the response to precipitation recharge. Numerous controls such as soil coverage, bedrock amounts, vegetation, and solar energy influx can be evaluated to determine their significance on the rates of evaporation and baseflow recession constants for various watersheds. These controls can interact with each other and affect evapotranspiration and baseflow recession constants to varying degrees. Some controls such as areas of vegetation coverage and solar energy influx are not easily measured in the field but can readily be determined using geographical information system (GIS) programs.

GIS programs facilitate the collection, visualization, manipulation, and analyses of spatially or geographically located data, which can then be used to determine patterns, relationships, and trends in the data. GIS can take seemingly unrelated data and allow analyses of that data using a common geographical location as the base reference point. Different GIS applications are available to process the data depending on what analysis is to be performed. My thesis applies a GIS approach to detailed comparison and analysis of two paired watersheds.

Purpose of the Project

The purpose of this project is to quantify hydrogeological, biological, and solar energy controls on differences in evapotranspiration and baseflow recession previously observed (Nourse et al., 1996, 2010) in two paired watersheds that feed San Antonio

Creek. Nourse et. al,1996, 2010 speculates that the differences seen in the evapotranspiration and baseflow recession constants are due partly to vegetation, rock and soil configurations, and sun exposure. Other researchers have also suggested that these differences may play a role but few comprehensive studies have been conducted in the watersheds.

Baseflow recession is a measure of watershed drainage that records the response of the watershed to precipitation recharge and subsequent discharge of water from groundwater loss. Possible controls on evapotranspiration rate and baseflow recession might be due to differences in soil vs. bedrock coverage, vegetation, solar influxes, and precipitation inputs. These differences will impact how much water is retained or released through evapotranspiration and may be observed in the baseflow recession constants. Other variables such as the amount of solar influx can be an important factor to consider as it will also affect how water moves in the watersheds. Varying amounts of soil and bedrock coverage should also affect groundwater infiltration and/or runoff rates.

Objectives of the Project

My objectives are to use GIS tools to map geographic variations in these parameters and quantify differences between the watersheds using tables, maps, and charts. My data set includes two previous geological maps of the area (Nourse, 1994; Nourse, personal communication) and a set of four geologic maps (Dibblee, 2002, 2003), a United States Geological Survey (USGS) Digital Elevation Model (DEM) raster data set obtained from the National Elevation Dataset (USGS), and a USGS Digital Raster Graphic (DRG) topographic map. In addition, I also utilize high

resolution Google Earth Pro™ satellite imagery to distinguish vegetation in remote areas. Mapped contacts are field checked and crossed referenced in a multi-layered GIS database. The ArcGIS (version 10.2.1) program facilitates calculations of areas, hill shade, slope angles, and sun angle distribution that yield comparisons of the watersheds.

Location of the Project

The two watersheds are located in the eastern portion of the San Gabriel Mountains directly north of Mt. Baldy village, California (Figure 1). The study area is bounded by the coordinates from 34.25° N to 34.125° S, -117.751° W to -117.626° E. Upper San Antonio Canyon (SAC) watershed is the larger of the two with an area of approximately 14.08 square kilometers (5.44 square miles), while Icehouse Canyon (IHC) watershed is somewhat smaller in size at approximately 11.89 square kilometers (4.58 square miles). Both watersheds exhibit steep, canyon walls with moderately incised stream channels. Elevations range from 1425 to 3068 meters (4750 feet to 10,064 feet) above mean sea level (AMSL) in the upper San Antonio Canyon watershed while the elevation ranges in Icehouse Canyon from 1425 to 2739 meters (4750 feet to 8986 feet AMSL). San Antonio Canyon has a predominant north-south trend, while Icehouse Canyon has an east-west trend. The median elevation for upper San Antonio Canyon watershed is at 2346 meters (7696 feet) while the median elevation for Icehouse Canyon watershed is at 2081 meters (6827 feet).

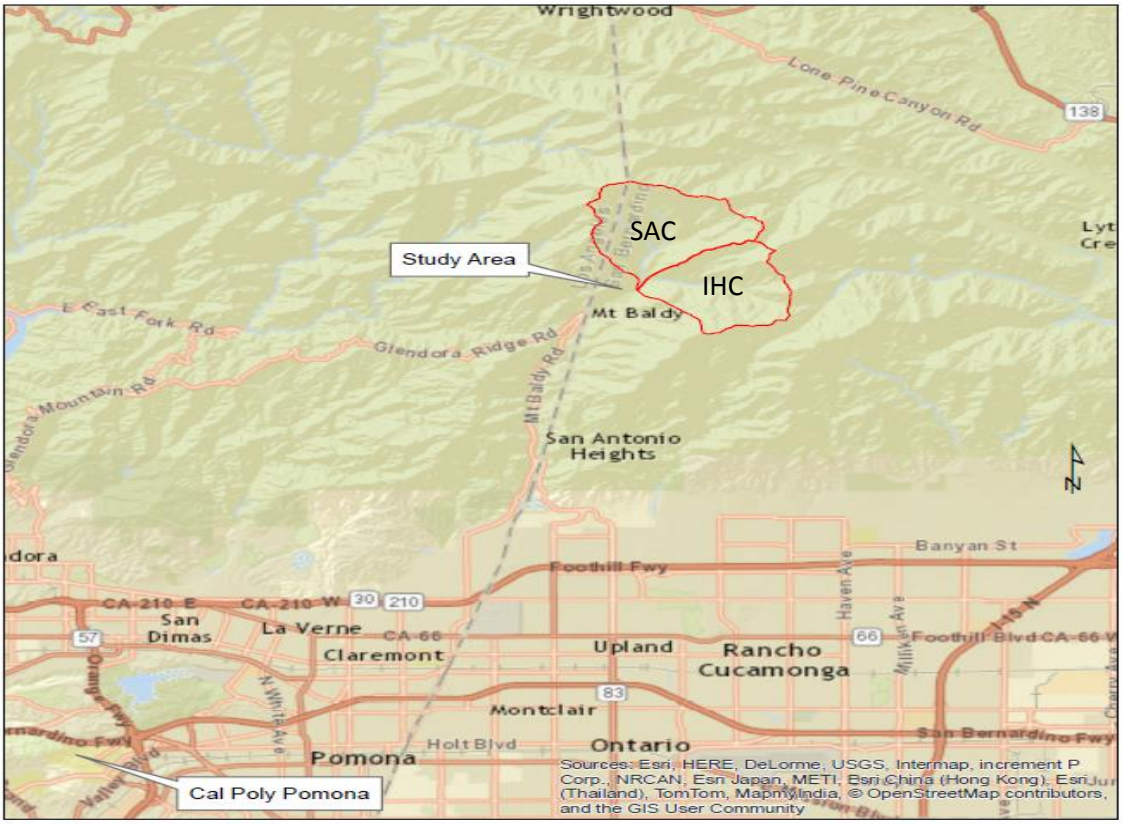

Figure 1. Location of study area. The upper San Antonio (SAC) and Icehouse Canyon (IHC) watershed boundaries are shown in red.

Hypotheses and Research Questions

I intend to test and refine general hypotheses or speculations (Nourse, 1996) that contrasting base flow recession constants and evaporation rates in these two watersheds are caused by different amounts of bedrock coverage, vegetation, and/or solar energy influx. Important questions that bear on this hypothesis include: (1) What percentage of bedrock vs. landslide vs. colluvium covers each watershed and are there any measureable differences? (2) Does the level of bedrock exposure correspond to any particular dip directions? (3) What type and variation of soils and vegetation exist? (4) Does the sun angle, hill shade, and/or faulting play a role in baseflow recessions? and

(5) What other possible controls are there on precipitation, runoff, and evaporation in the watersheds?

GIS Approach to this Project

Geospatial data is commonly obtained and digitized from a variety of sources that include paper maps, satellite imagery, and aerial photographs. GIS programs allow digitization of features directly on top of an image or scanned paper map generally referred to raster images. The raster map or image must first be geographically referenced in order to perform any meaningful analysis. Once georeferencing is accomplished, it is relatively straightforward to digitize data. Georeferencing is the process of taking a paper raster map or document, locating four or more distinct points, and then matching these same points on a base map that has an existing geographical coordinate system. Data is then stored in a standalone file or more commonly stored in a geodatabase file. Different types of analyses can later be performed on these data files as needed.

Digitized data is made up of a collection of points, lines, or polygons. These represents either a two or three dimensional object located on the earth's surface. Points and lines generally represent discrete items such as trees and streams while polygons typically represents surface areas such as soil units. Points, lines, and polygons are grouped separately and make up a geographical data layer or feature. Features can then be combined and layered on top of each other to make a map (Figure 2).

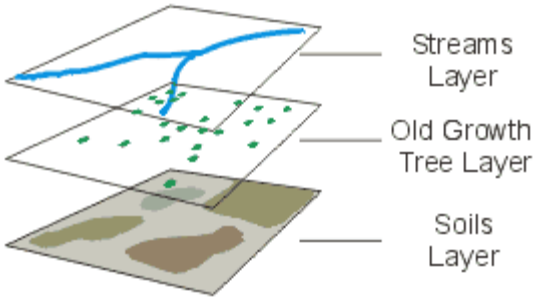

Figure 2. Map data layers (from www.willcogis.org).

Another important feature of digitized data that needs to be considered is map topology. Topology is a mathematical set of special rules on data geometry stored in a database that is used to enforce certain database processes and how data is displayed on a digital map. Map topology represents spatial objects (points, lines, polygons) as nodes, edges, and faces that can be stored in a database with geographical coordinates (Figure 3).

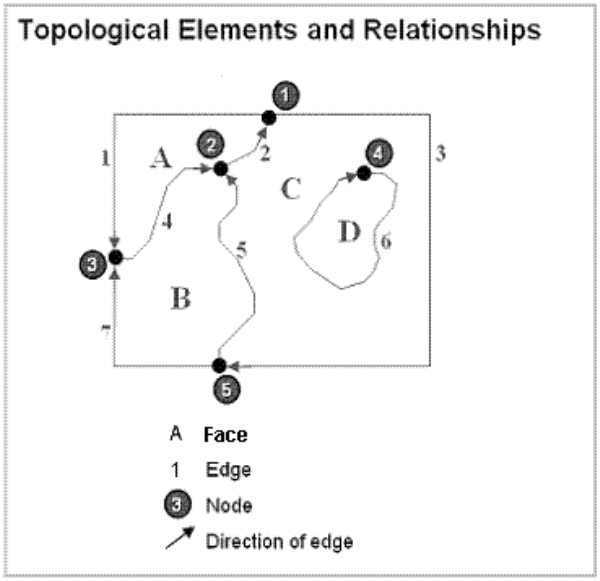

Figure 3. Topologic elements (from ESRI.com).

Topological rules can be set up in GIS programs to flag potential errors in the data and allow the GIS user to correct the errors. Properly applied, map topology ensures data integrity by minimizing erroneous data entries. For example, some types

of data share boundaries such as two features, a stream and a bedrock outcrop. Each feature has a distinct boundary which is represented on a map as a line edge. Rules are applied and enforced to these two features such that they cannot have any gaps or overlaps in the digitized data but can share edge boundaries. By using topology, maps that are made should be error free or "topologically clean".

CHAPTER 2

GENERAL HYDROLOGICAL BACKGROUND

Climate, Hydrology, and Local Geology

Upper San Antonio and Icehouse Canyons watersheds(Figure 1), located in Southern California, have a semi-arid, Mediterranean-type, regional climate characterized by hot, dry summers and cool, mild winters which allow for certain plant relationships to develop (Rundel and Gustafson, 2005). Winters are punctuated by periodic rain fall during the rainy season from October to June with snowfall only occurring in the higher elevations. Snowpack seldom persists beyond the early spring months with some rare exceptions on north facing slopes during high precipitation years. The intensity of rain fall recorded over a 115 year period at Sierra Powerhouse in lower San Antonio Canyon, elevation 950.9 meters (3120 feet) varies from year to year and can range from a low of less than 25.4 centimeters (10 inches) to an average mean precipitation rate of approximately 78.8 centimeters (31 inches) with several recorded highs in excess of 152.4 centimeters (60 inches). Precipitation records are generally incomplete for the actual study area; however, some limited records exist for Icehouse Canyon receiving approximately 101- 114 centimeters/yr (40-45 inches/yr, Nourse, unpublished data). Nourse's values are based on water budgets developed for the eastern San Gabriel Mountains by Troxell, (1958).

Mediterranean climates can be found between the latitudes 30-45 degrees North and South of the equator. Less than three percent of the world surface has this type of climate (Quinn and Keeley, 2006). Both of the canyons contain evergreen shrub vegetation typical of a Mediterranean climate. Three factors are responsible for this

unusual climate; a cold ocean nearby, the latitude, and the onshore, high pressure air mass known as the Pacific High which moves depending on the season (Quinn and Keeley, 2006). During the winter months when the Pacific High moves southward, the region experience rain fall from storm systems originating in the North Pacific. In the summer months the Pacific High is especially strong and remains parked over the region thus preventing storm systems from entering the region. It is only when the Pacific High is disturbed or weakens, that the region may experience rainfall.

Microclimates also exist in the canyons depending on several factors. Slope direction, deep ravines, and sun angle are some of the factors which influences local climate and hence affects how water is released or retained (Quinn and Keeley, 2006). Deep ravines typically shade the local vegetation from the sun. Depending on the direction the slope faces such as a north facing slope and the angle of the sun above the horizon, deep shade may develop in some of the canyons. Temperatures in these areas are also moderated with less variation in temperature throughout the day due to less solar insolation being received and heating up the ground surface (Quinn and Keeley, 2006). This in turn results in an overall decrease in soil moisture evaporation enabling plants to better tolerate drought conditions. In those areas that have less sun exposure, the vegetation tends to be thicker and more vigorous than on the more exposed slopes.

Distinct microclimes may develop causing some slopes to develop one predominant vegetation type depending on the direction the slope faces (Rundel and Gustafson, 2005). Chamise (*Adenostoma fasciculatum)*, a shrub commonly found in the San Gabriel Mountains, favors dry, south facing slopes forming dense thickets. Oaks, which prefer more moisture, will tend to be found on north facing slopes. By

determining the overall predominant vegetation present, this can be a very good indicator of the local microclimates in the canyons and the available soil moisture for vegetation.

Water flow in the upper San Antonio and Icehouse Creeks is dependent on the annual precipitation received and the discharge from numerous springs located throughout the watersheds. Enhanced water flow occurs during precipitation events and will vary according to the strengths of the storm systems. The fact that there is strong water flow in both the creeks year round during extended dry periods indicate there are significant contributions from groundwater sources (Nourse, 1994) in addition to the precipitation inputs. Some stream segments, however, do have large amounts of unconsolidated alluvium that act as sponges causing those segments to go dry. Quaternary alluvial deposits are found in the creeks to varying thicknesses with crystalline bedrock material below the alluvium acting as a subsurface control on the surface water flow.

Previous Works

It is well known that geomorphology, land use, geology, vegetation, temperature, and precipitation/evapotranspiration rates all influence baseflow recessions (Price, 2011). Few comprehensive investigations have been conducted of the two watersheds. Of the previously published works on San Gabriel Mountains hydrology (Vathanasin, 1999; Strand, 2006; Carey, 2009; Nourse, 1994, 2010), researchers have posited the possible influences that vegetation, soil coverage, faulting, and solar influx might play on baseflow recessions. Most of the studies mention the various controlling

factors; however, none of the studies actually present data on the various environmental factors that I will be addressing.

Several early hydrology works from the study area reported stream gauging results and geological mapping in Icehouse and Upper San Antonio Canyon conducted by Jon Nourse and various students from the Cal Poly Pomona Groundwater Geology class (Vathanasin, 1999, Strand, 2006, Carey, 2009, Nourse, 1994, 1996). Two publications are especially pertinent to this current study: A technical report to a local homeowner's association (Nourse, 1994) describes the location of springs in Upper San Antonio Canyon and detailed hydrogeologic mechanisms for their existence. This report is the source of the geologic map reproduced and digitized below (Figure 10). A Geological Society of America abstract (Nourse et al., 1996) compares the water budgets of Upper San Antonio watershed with Icehouse watershed, reports evapotranspiration rates of 55% and 45% respectively, and postulates reasons for these differences. Ideas presented in that abstract are tested and addressed in detail below.

Vathanasin (1999) analyzed and discussed the water budget for the San Dimas Experimental Forest (SDEF) in the San Gabriel Mountains consisting of two local watersheds, the Big Dalton and San Dimas, located to the southwest of the upper San Antonio and Icehouse Canyon watersheds. The SDEF watersheds are much lower in elevation than the Upper San Antonio and Icehouse Canyons watershed. Vathanasin's focus was on the historical precipitation, runoff, and evapotranspiration values based on precipitation data from numerous stream gages located in the SDEF. Vathanasin determined that both the Big Dalton and San Dimas watersheds have an evapotranspiration rate of approximately 84%, and suggested that vegetation plays a

role in the overall evapotranspiration rates observed the SDEF. These watersheds also have a Mediterranean type climate and have similar chaparral vegetation to that seen in the upper San Antonio and Icehouse Canyons. However, cursory inspection of photographs from the area suggest a lower proportion of conifers.

Strand (2006) also studied and discussed the possible controls on evapotranspiration in the SDEF. Her study specifically looked at the role that various controls may play in the SDEF after fire events. She mentioned that geology, vegetation, and sun exposure may have a potential effect on the baseflow recession rates calculated for the SDEF. She compared the baseflow recession rates of Icehouse Canyon and San Antonio Canyons based on analysis by Vathanasin and Nourse to her study area as the geology, vegetation, and climate are similar. Her study calculated the baseflow constant for the different creeks studied in the SDEF. She determine for Wolfskill Creek to be 0.019 $days^{-1}$, 0.0320 $days^{-1}$ for the Middle Fork San Dimas Creek, and 0.0.0246 $days^{-1}$ for the East Fork San Dimas Creek (Table 1). She suggested that sun exposure may have the greatest influence on evapotranspiration rates and stated that this may also account for the differences in the baseflow recession constant seen in the upper San Antonio and Icehouse Canyons. Her assumptions are based on the differences in baseflow recession constant; however, the focus of her study was primarily on the effects of fire damage and presented no data on vegetation amounts or sun influx rates to support her assumptions.

Carey (2009) analyzed the spring discharge rates in Icehouse Canyon to determine the changes to the baseflow recession constant of Icehouse Canyon. She

calculated the baseflow recession constant for San Antonio and Icehouse Canyons to be 0.0185 $days^{-1}$ and 0.0081 $days^{-1}$ respectively (Table 1).

TABLE 1. SUMMARY OF BASEFLOW RECESSION CONSTANTS

Location	Baseflow Recession Constant (days-1)
Wolfskill Creek (SDEF)	0.019
Middle Fork (SDEF)	0.032
East Fork (SDEF)	0.0246
Upper San Antonio	0.0185
Icehouse Canyon	0.0081

Adapted from Carey, 2009

Her findings suggested that the constants clearly vary and are a reflection of multiple factors influenced by the topography, local geology, sun angle (solar insolation), temperature, and transpiration. Her study concluded that these variables could possibly be applied to other local watersheds including upper San Antonio. She also states based on her analysis that the landslide material in Cedar Canyon is a good aquifer due to its permeability and its tendency to retain water, slowly releasing it over time and hence influences baseflow recession constants.

Nourse et. al. (2010) present detailed analyses on numerous, perennial springs located in both watersheds. Evidence is presented for differences in the baseflow recession between the two watersheds (Figure 4). They suggest that the baseflow recessions are due in part to specific geologic controls including spring discharge from water saturated landslide material, infiltration of water into fault bounded gravel deposits, and water flow in areas with bedrock constrictions of alluvium. Possible mechanisms related to vegetation differences and sun angle are also mentioned, but not supported with data.

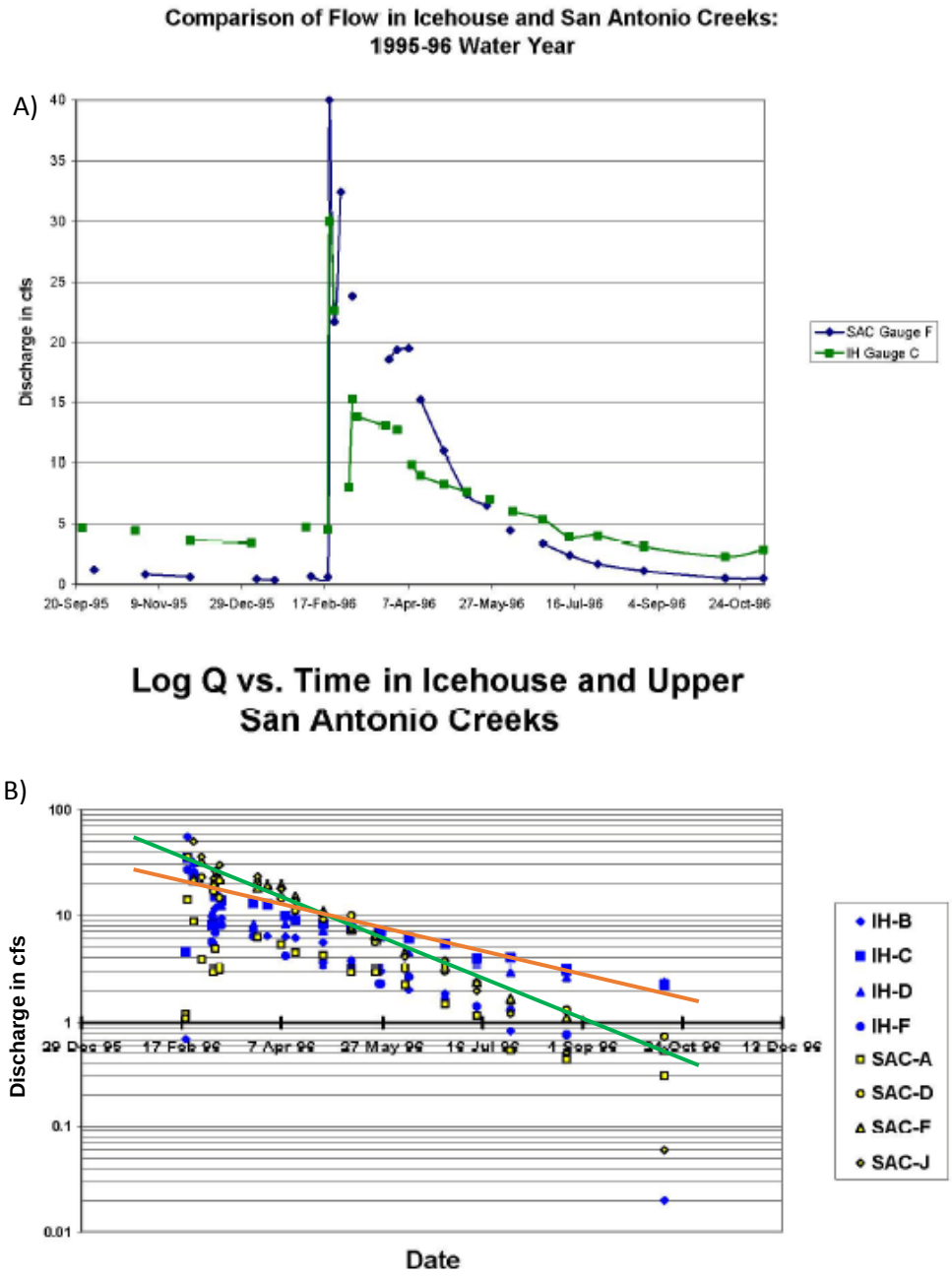

Figure 4. Hydrograph comparison of flow between Icehouse Creek and San Antonio Creek during the 1995-1996 water year (A). The second graph (B), is the same data plotted logarithmically. The green line represents the baseflow recession for upper San Antonio Creek; the orange line represents the baseflow recession for Icehouse Creek. The different slopes imply differences in the discharge rates for the watersheds. Adapted from Nourse et al., 2010.

CHAPTER 3

METHODOLOGY

ArcMap 10.2.1 GIS software was obtained from Environmental Systems Research Institute (ESRI) and was used to develop all maps and graphs used in this study. A student copy was obtained from ESRI free-of-charge with a one year license that contains ArcMap, the basic map making component, and all tools used for data processing. Three levels of licensing are available: Basic, Standard, and Advanced. ArcMap Advanced was used for the study as it has the most data processing capabilities available including topological rules. An example of the type of product generated by the program is shown in Figure 5.

All data used in the project was converted to the North American Datum of 1927, Clarke 1866 spheroid geographic coordinate system (NAD 1927 or NAD27). Geographic coordinate systems are based on mathematical models of the shape of the earth and are used to define the location of features on the earth's surface. Some models use a perfect sphere as the basis for the geographical coordinate system while most others use an oblate spheroid as the base model. Because the earth is not a true sphere but bulges somewhat at the equator, the spheroid will have both a major and a minor semi-axis (Figure 6).

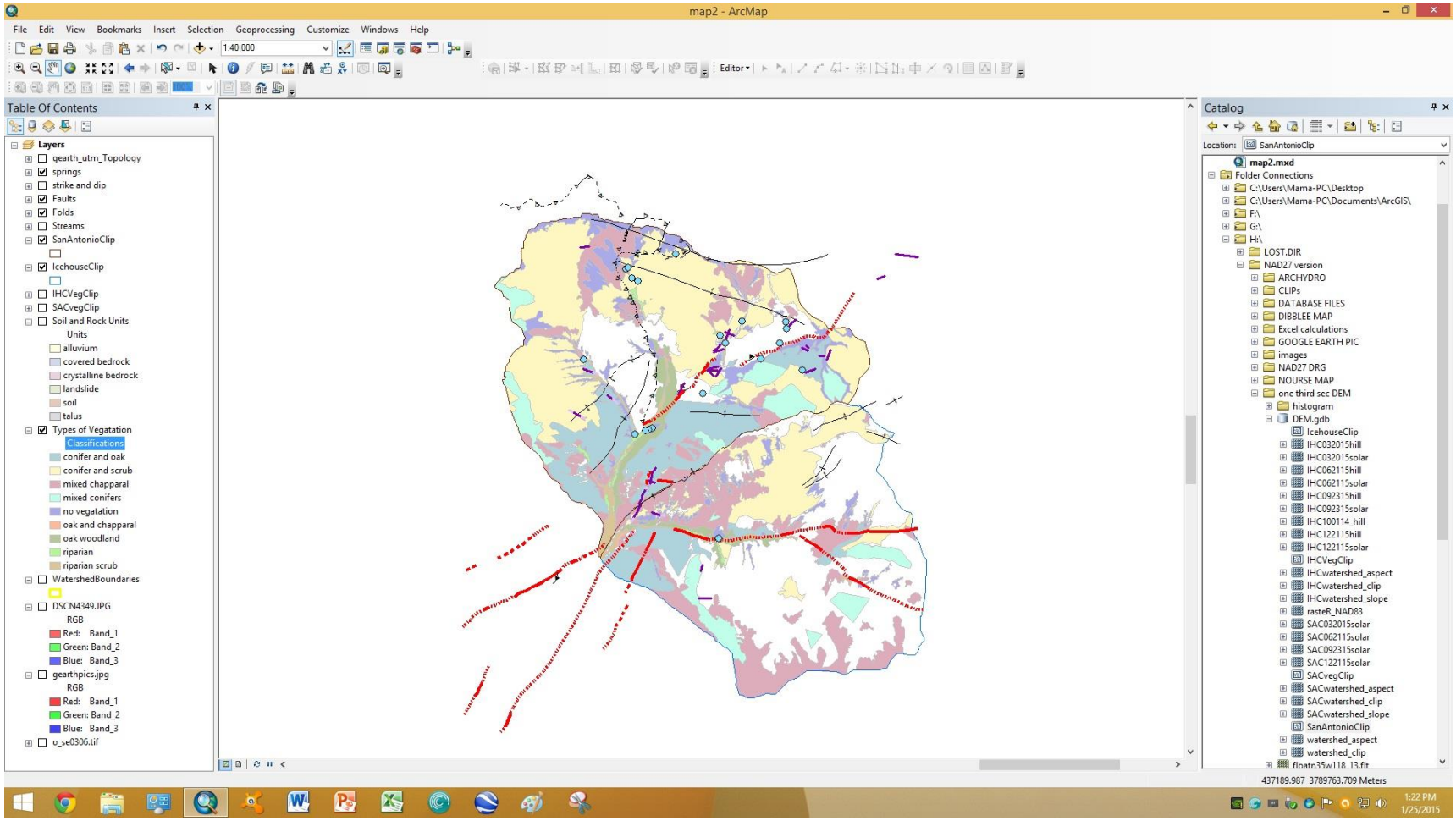

Figure 5. Screen shot of the ArcMap program. Vegetation units, spring locations, faulting, and folding are shown on the map.

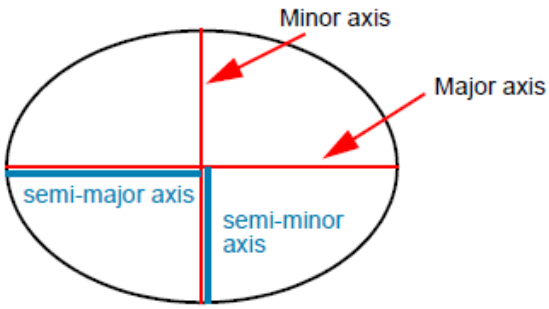

Figure 6. Diagram showing a spheroid.

The difference occurring in the datums is a result of how the semi-major and semi-minor axes are measured and is dependent on the initial starting reference point (Figure 7).

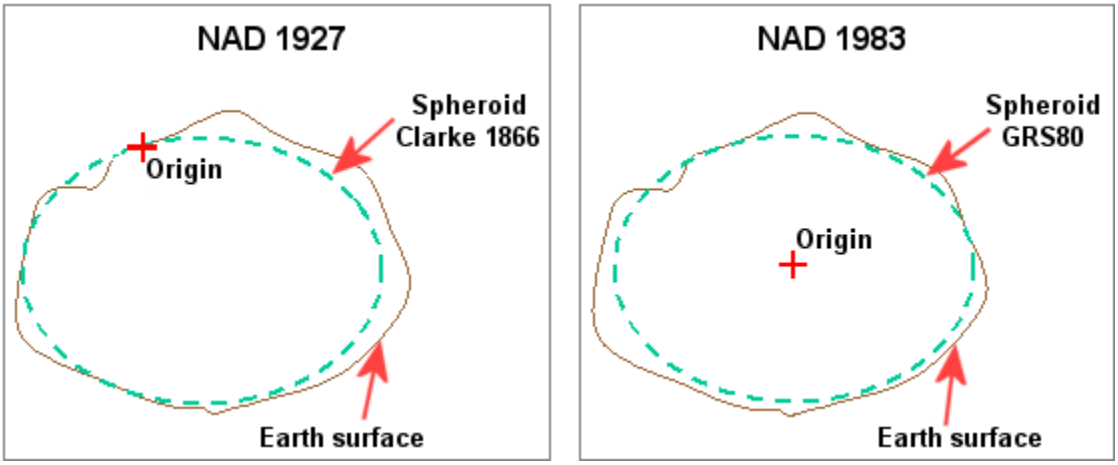

Figure 7. Diagram showing the differences between commonly used datums.

From the measured ellipsoid, latitude and longitude along with altitude are determined which defines the datum. NAD27 uses a local survey point, surface based measurement taken at Meades Ranch back in 1927 and uses the Clarke 1866 spheroid model as the basis for the datum. Every other point in that datum was subsequently surveyed in North America based off this surveyed benchmark taken at Meades Ranch until newer more refined datums became available. This datum probably best represents the shape of the earth for North America as it is based on local surveying

whereas other models use an overall general best fit for the spheroid. NAD 1983 (NAD83) uses an earth centered measurement for its datum and has begun to replace NAD27. Datums have now become much more accurate with the advent of global positioning systems (GPS) measurements. The NAD27 datum was selected since large amounts of data are still available in NAD27 and continue to be commonly used by geoscientists.

Data transformations are necessary to prevent alignment shifts in the data (Maher, 2010). NAD27 differs from NAD83 by a distance of approximately 47.2 meters (155 feet) on the east coast of the United States. The difference decreases westward to approximately 22.8 meters (75 feet) in the Midwest then increases again westward to approximately 91.4 (300 feet) on the west coast. Transformations can also be performed to change from a geographic coordinate system to a projected coordinate system. For the study project, a projected coordinate systems is needed in order to represent a three dimensional shape in a two dimensional form. This operation was necessary in that areas cannot be accurately measured in a geographical projection system which typically uses decimal degrees. One degree of angle will have a different actual area measurement as the angle is measured from the equator to higher latitudes.

Projected coordinate systems allow areas to be measured accurately using linear units such as feet or meters. All data that was obtained in a different datum was transformed to a NAD27 Universal Transverse Mercator (UTM) zone 11, a common projected coordinate system. The projected UTM system used divides the world into 60 equal zones of six degrees of longitude with twenty bands of eight degrees latitude forming an overall grid pattern of the earth (Figure 8).

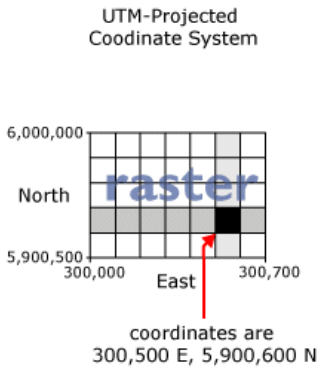

Figure 8. Diagram showing UTM coordinates.

Data used in the study was obtained from a variety of sources. The Dibblee map (Figure 9) is comprised of four different 7.5 minute quadrangles (Dibblee, 2002, 2003) that were joined together using Adobe® Photoshop® from electronic files purchased and downloaded from the American Association of Petroleum Geologist (AAPG) organization. The quadrangles sheets obtained were the Mt. Baldy, Cucamonga Peak, Telegraph Peak, and Mt. San Antonio quadrangles. The 7.5 minute quadrangles were trimmed of all extraneous information and then joined to form one large file saved as a portable document format (pdf). This file was then imported into ArcMap for georeferencing.

Georeferencing is the process of taking a paper map or document which has been electronically scanned, locating four or more distinct points, and then matching these same points on a base map that has an existing geographical coordinate system. This process assigns the same coordinate system to the scanned document as the base map. Because the scanned image is stretched to meet the four reference points there are some problems encountered with this technique. Alignment issues can develop if the image is stretched over relatively large distances such as four quadrangles and the control points on the image are hard to exactly locate on the reference map. There were

fewer alignment problems with the Dibblee map since the Dibblee map is based on a topographic map and control points were easier to locate.

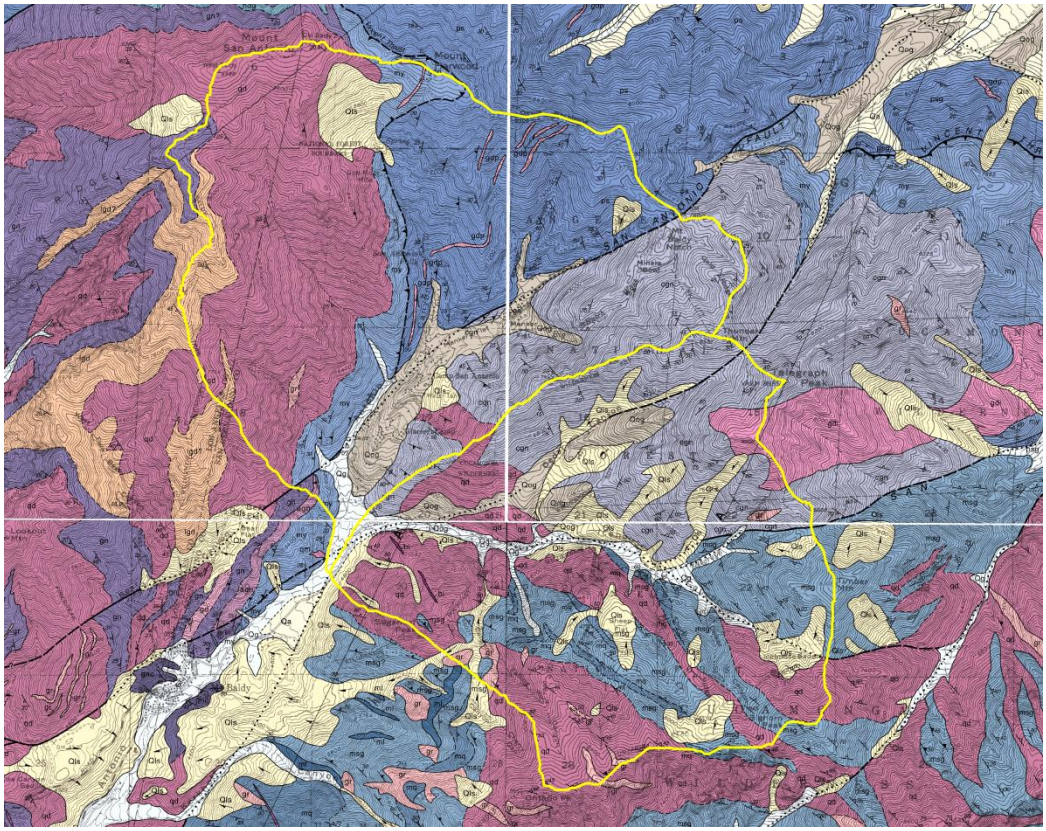

Figure 9. Original Dibblee maps. The Dibblee 7.5 minute quadrangles are joined together. Note that the quadrangles do not completely align together. The yellow line represents the two watershed boundaries. This is the base map used for digitization (Dibblee, 2002).

An electronic raster file of the Nourse et al. (2010) map (Figure 10) was obtained from Dr. Jonathan Nourse. The file was imported into ArcMap and subsequently georeferenced to a topographic DRG map of the study area. The four quadrangles were initially joined together in the same fashion as the Dibblee map; however, upon georeferencing, it was noted that a more accurate overlaying of the map could be obtained by georeferencing each individual quadrangle as more control points could be used during the georeferencing operation.

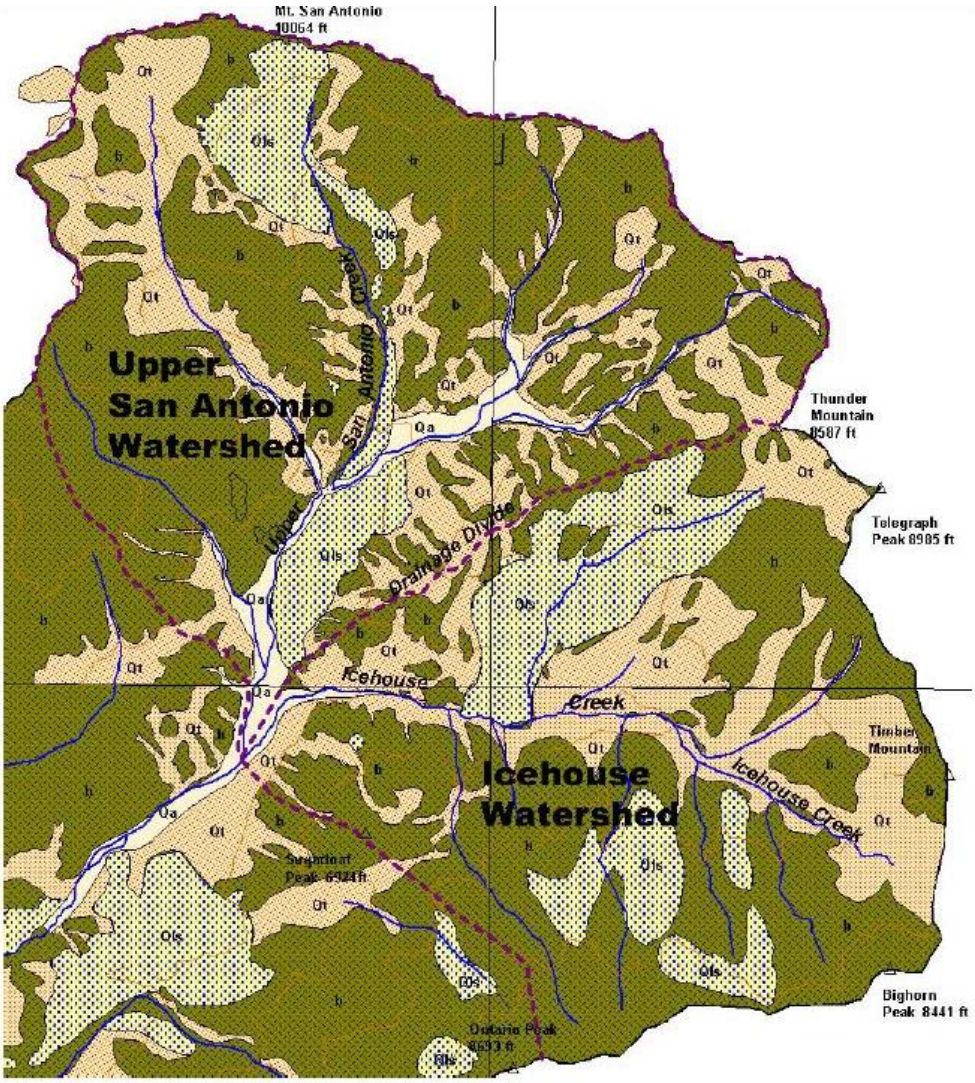

Figure 10. Original Nourse geologic map. The various rock and soil units used in the study are shown. Note that the 7.5 minute quadrangles are not exactly aligned. Qls= Quaternary landslide deposits, Qt = Quaternary talus deposits, Qa = Quaternary alluvial deposits, b = crystalline bedrock The Upper San Antonio Canyon watershed map was first published in a technical report (Nourse, 1994); hydrogeology of Icehouse Canyon watershed was published in Nourse et al., 2010.

A more detailed series of structural geological maps were obtained from Dr. Nourse (unpublished data 1991-2004). These showed the regional structural geology of the study area, with strike and dip readings, faults, and folds and additional information such as spring locations. The maps were used for the structural information and

georeferenced in the same manner as the other maps. Structural information was digitized then incorporated into the Google Earth™ portion of the data analysis.

For the satellite image portion of the study a Google Earth Pro™ satellite image was obtained from Google Earth™. The study area was first roughly determined then a series of six high resolution images were saved as pdf files. The images, which contained the Google Earth™ logo, were cropped and edited in Adobe® Photoshop® to remove the logo and to join together the six images to form one composite image (Figure 11).

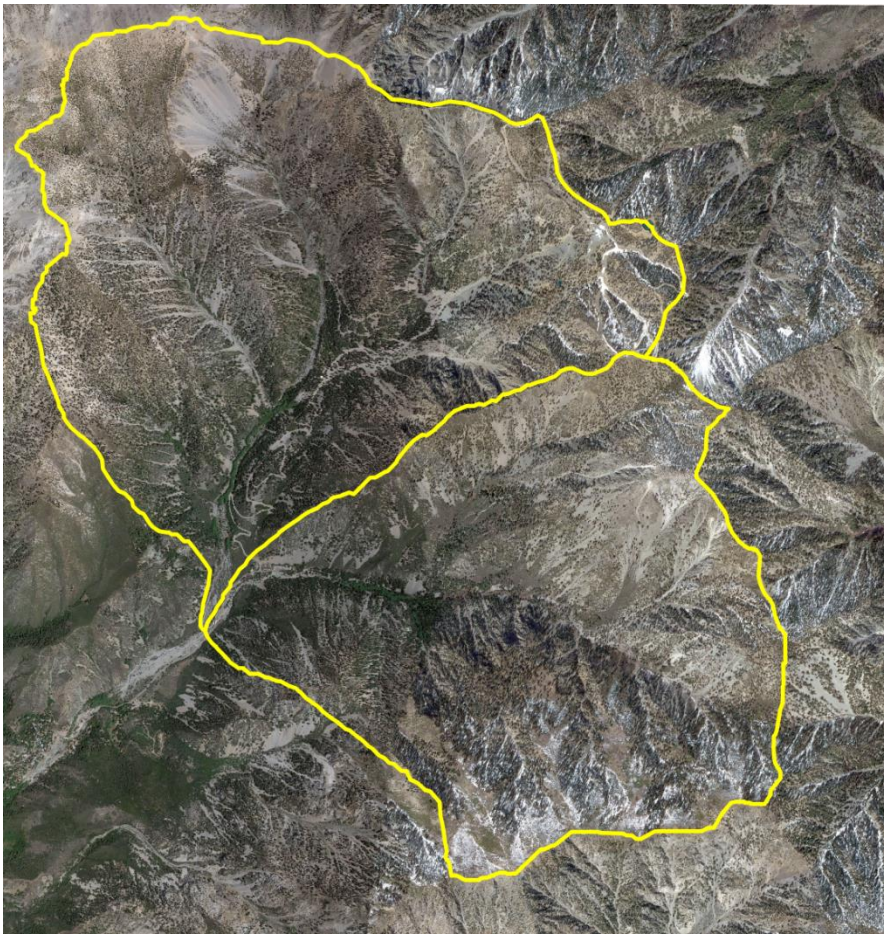

Figure 11. Google Earth™ composite image. Landsat image data. The yellow boundary represents the two watersheds. Google and the Google logo are registered trademarks of Google Inc., used with permission.

The composite satellite image was converted from WGS 1984 (WGS84) Web Mercator to NAD27 using ArcMap's geographic transformation process. The image must be transformed in order to prevent alignment problems with other data used in the project. Web Mercator projections produce lines that intersect all meridians at the same angle thereby distorting both distances and areas. The date of the image used is 3/21/2013 taken during the spring months with minimal snow cover present.

DEM raster data was requested using the study boundaries and obtained from the USGS National Elevation Dataset (NED) as a compressed, mosaic raster data set. Raster data is a type of data composed of a matrix of cells organized into rows and columns containing spatial, spectral, or temporal information. Each cell represents some value at a particular spatial location (Figure 12) such as temperature, elevation, vegetation type, etc.

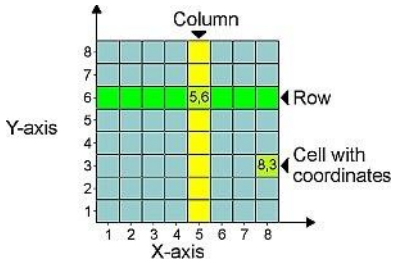

Figure 12. Diagram showing raster structure.

Scanned documents, aerial photographs, and satellite imagery are typically stored as a digital raster data file.

Data is available in 1-arc second (30-meter resolution), 1/3 arc-second (10-meter resolution), or 1/9 arc-second (3-meter resolution). One third arc-second data was requested and received courtesy of the U. S. Geological Survey. A compressed file was received in a GRID FLOAT format which can be directly used in ArcMap. The

compressed files were extracted, added to ArcMap and transformed from NAD83 to NAD27. Because the data files are extremely large, a portion of the data called a clip was taken using the watershed boundaries from the Nourse map in order to reduce the overall file size and decrease the time to process the data for aspect, hill shade, and solar insolation determinations using the geoprocessing tools available in ArcMap. Hill shade and solar insolation maps use sun azimuth and altitude to predict the solar insolation values received in the canyons for the 2015 year.

Vegetation units were based on the predominant types of vegetation seen on the imagery or noted during field checks conducted throughout the two watersheds (Table 2). Many different types of vegetation can be found occurring together because of the local microclimates present. Elevation also plays a factor in the location of various plants. For example, limber pines (*Pinus flexilis*) will only grow above 2130 meters (7000 feet) yet depending on the species, manzanita (*Arctostaphylos sp.*) can be found at all elevations throughout the watersheds.

Soil units, i.e., landslide (Qls) vs. talus (Qt) vs. alluvium (Qal), were kept the same for both the Dibblee and Nourse maps while two additional units were added to the Google Earth™ map; a "covered bedrock" unit and a "soil" unit. The covered bedrock unit was used for those areas that were located adjacent to exposed crystalline bedrock but had little or no exposed bedrock and are in areas that have slopes greater than twenty degrees. No depth to bedrock could be determined; however, most mountainous areas have thinly bedded mantles of soil. The soil unit was used as generic unit for those areas in which there was no clear indication of the original

material present, have slope angles less than twenty degrees, and could not be readily classified into one of the other units.

TABLE 2. VEGETATION UNITS

Unit	Common Plant Species	Description
Riparian	White alder *(Alnus rhombifolia)*	Deciduous tree found in creek bed; high water demand
	Western sycamore *(Plantanus racemosa)*	Semi-deciduous tree found in creek bed
	Big leaf Maple *(Acer macrophyllum)*	Deciduous small tree found on creek sides
	California bay laurel *(Umbellularia californica)*	Evergreen small shrub-tree found on creek
	Incense Cedar *(Calocedrus decurrens)*	Evergreen tree found on creek sides
	Berry *(Rubus sp.)*	Semi-deciduous bush on creek sides in moist areas near springs
	Willow *(Salix sp.)*	Evergreen bush found in creek bed; high water demand
Riparian scrub	California buckwheat *(Erigonum fasciculatum)*	Evergreen shrub
	Mule fat *(Baccharis salisafolia)*	Evergreen shrub
	Yucca *(Yucca whipplei)*	Evergreen shrub
Mixed Chaparral	Manzanita *(Arctostaphylos sp.)*	Evergreen shrub
	Mountain mahogany *(Cerocarpus betuloides)*	Deciduous shrub to small tree
	Spiny redberry *(Rhamnus crocea)*	Evergreen shrub
	Scrub oak *(Quercus berberidifolia)*	Evergreen shrub
	Sugarbush *(Rhus ovata)*	Evergreen shrub
	Laurel sumac *(Malosma laurina)*	Evergreen shrub
	Lemonadeberry *(Rhus integrifolia)*	Evergreen shrub
	Bush monkey flower *(Mimulus aurantiacus)*	Evergreen shrub found on dry slopes
	Flannel bush *(Fremontodendron californicum)*	Evergreen shrub found on dry, granitic slopes
	Yucca *(Yucca whipplei)*	Evergreen shrub
	Sage *(Salvia sp.)*	Evergreen shrub
	California buckwheat (*Erigonum fasciculatum*)	Evergreen shrub
	Mountain lilac *(Ceanothus sp.)*	Evergreen shrub
Oak Woodland	Oak (*Quercus sp.*)	Found along creeks but not in stream beds; generally canyon live oak *(Q. chrysolepis)*
	Poison oak (*Toxicodendron sp.*)	Deciduous shrub found in oak groves
Oak and Chaparral	Oak (*Quercus sp.*)	Semi-deciduous to deciduous tree
	California buckwheat (*Erigonum fasciculatum*)	Evergreen shrub
	Mountain mahogany (*Cerocarpus betuloides*)	Evergreen shrub
	Manzanita (*Arctostaphylos sp.*)	Evergreen shrub
Conifers and Oaks	Fir (*Albes concolor)*	Evergreen tree typically above 1828 meters
	Pine (*Pinus sp.*)	Mixed pines including Jeffrey, Coulter, Sugar, Yellow, and Lodgepole trees
	Oak (*Quercus sp.*)	Typically canyon live oak (*Q. chrysolepis*) and scrub oak (*Q. berberidifolia*) species
Mixed Conifers	Pine (*Pinus sp.*)	Mixed pines including Jeffrey, Coulter, Sugar, Yellow, and Lodgepole trees
	Big-cone spruce *(Pseudotsuga macrocarpa)*	Evergreen tree found from 610 meters to 2130 meters
Conifers and scrub	Pine (*Pinus sp.*)	Mixed pines including Jeffrey, Coulter, Sugar, Yellow, and Lodgepole
	Manzanita (*Arctostaphylos sp.*)	subalpine plants typically found above 2130 meters

CHAPTER 4

GEOGRAPHICAL INFORMATION SYSTEMS (GIS) DATA ANALYSIS

In the sections presented below, various pertinent analyses are presented that possibly affect the various controls on the evapotranspiration and baseflow recession. Three independent data sets of bedrock vs. soil distribution are digitized. Vegetation is subdivided and digitized. DEMs are analyzed for slope, aspect, and its derivative controls on hill shading and insolation. All digital files used in the analyses are available on DVD and are included. In addition two large format plates of the digitized Google Earth™ maps are located in the supplementary packet of this thesis (Appendix A, Plates I, II).

Analysis of the Dibblee Map

The watersheds as mapped by Dibblee (2002, 2003) consist of four main rock units: Quaternary alluvial deposits (Qal or Qa), Quaternary talus material (Qt), Quaternary landslide deposits (Qls), and Mesozoic crystalline bedrock (b). These units are used throughout the study for consistency although it can be seen in Figure 9 that Dibblee has subdivided many different rock units making up the crystalline bedrock used in this analysis. Plutonic and metamorphic rocks found in the area include biotite-hornblende granodiorites, leucocratic biotite granites, gneisses, mylonites, and schists. These were combined to form one crystalline bedrock unit (b). Since the focus of this study is not dependent upon the type of crystalline rock present, the combining was done in order that there could be a direct comparison between the digitized Dibblee, Nourse, and Google Earth™ maps (Figure 13).

Dibblee does not have a specific talus unit defined. For the purpose of this study, the unit marked by Dibblee as Quaternary old gravel (Qog) was digitized as talus material as Nourse (1994) and Nourse et al., (2010) have mapped this unit as Qt based on direct field observations in the canyons. Both correspond well to the Google Earth™ image for talus. The Dibblee map upon digitization shows a remarkable lack of detail but is useful for comparison purposes with the Nourse and Google Earth™ maps.

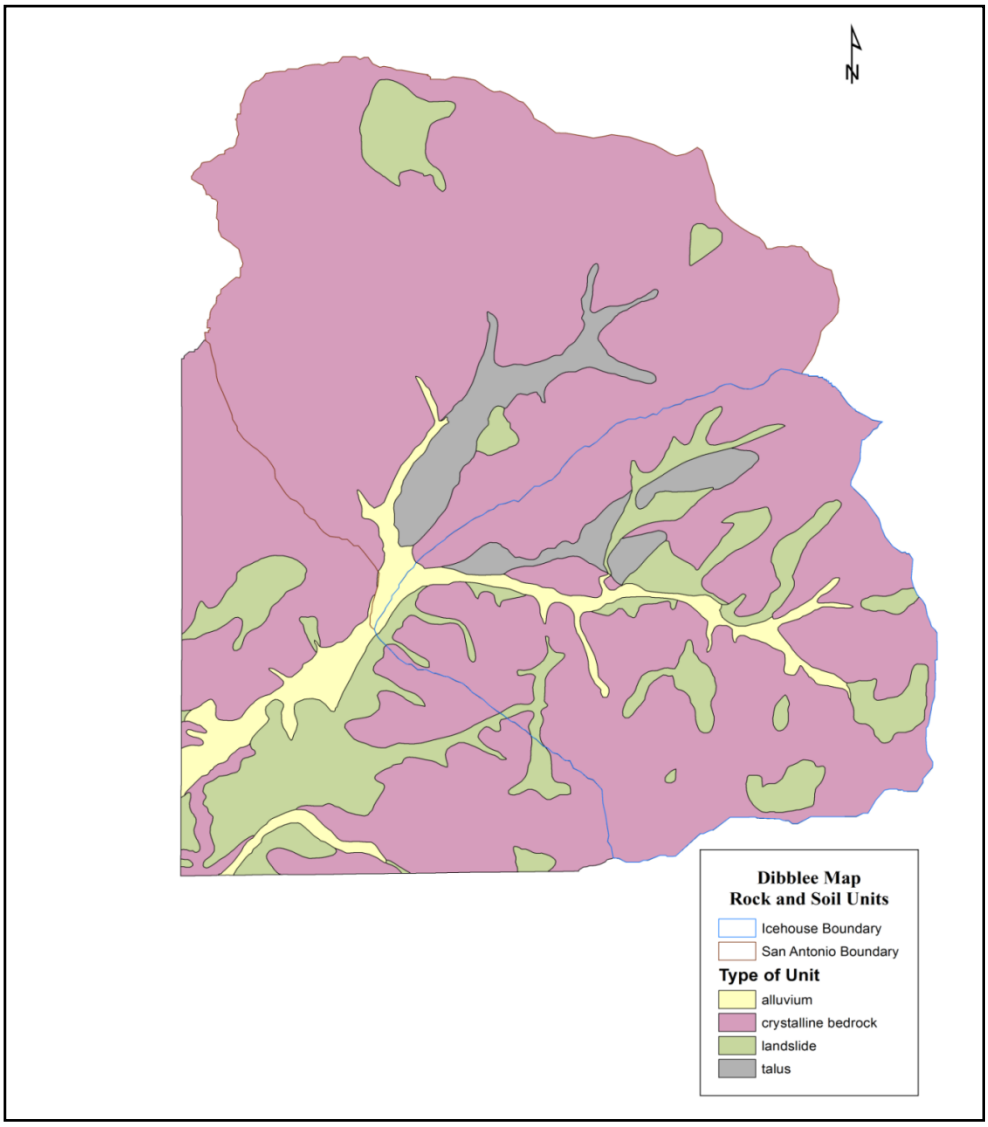

Figure 13. Digitized version of the Dibblee map derived from the composite image of Figure 9. The bedrock units were lumped together to better correspond with Nourse's map (Figure 14).

Analysis of the Nourse Map

The Nourse map (first published in its entirety in Nourse et al., 2010) is also a compilation of the four same 7.5 minute quadrangles used in the Dibblee analysis. The map is much more detailed in respect to the amounts of talus (Qt). Differences in the location and amounts of landslide material are evident between the Dibblee and Nourse maps. Interpretations of boundaries on the Dibblee map are most likely based on aerial photography and some field work while the Nourse map is based primarily on field work conducted by Nourse. A more detailed version of the Upper San Antonio watershed and part of Icehouse watershed, including strikes and dips of bedrock foliation and locations of perennial springs, was published in an earlier technical report (Nourse, 1994).

The digitized map (Figure 14) also contains the same units that were used during the digitization of the Dibblee map. A consistent color scheme was used in all of the digitized maps for ease of comparison between them.

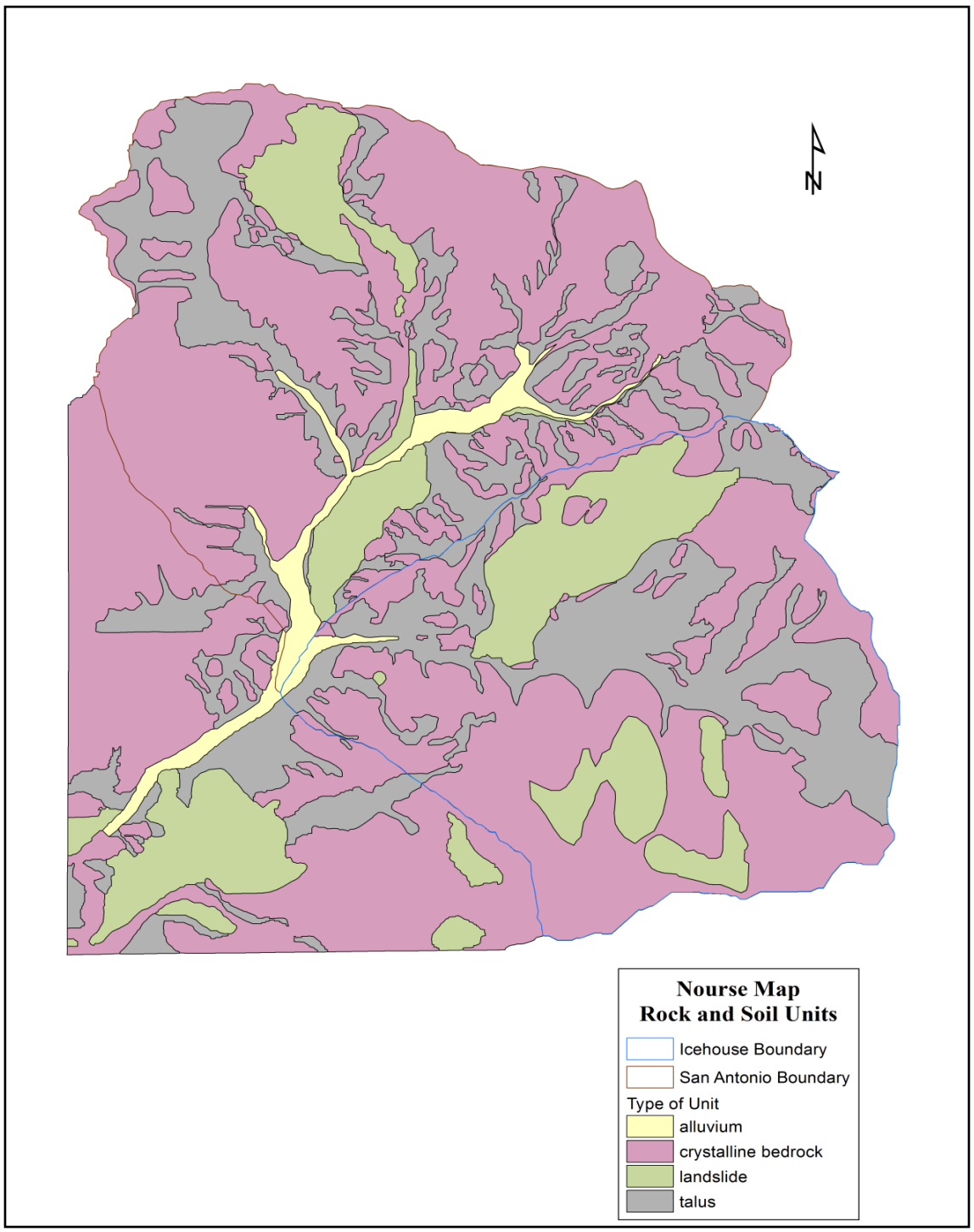

Figure 14. Digitized Nourse map used for the data analysis. The same rock and soil units were used as the original Nourse map (Figure 10).

Google Earth™ Satellite Analyses

Bedrock- Soil Analysis

The rock and soil map (Figure 16) was first digitized on the Google Earth™ image then a separate map was made with the vegetation units digitized (Figure 17). The watershed boundaries were imported from the Nourse digitized map in order to keep the areas consistent throughout the study. In studying the composite satellite image it was readily apparent that the four main rock and soil units used in the Dibblee and Nourse maps would not be sufficient for the analysis. Two additional units, a covered bedrock and a soil unit, previously discussed were used for those areas that could not be classified in the original four units. This was necessary because of the apparent correlation between the vegetation and the rock/soil present within the watersheds that were visible on the satellite image.

Some problems were encountered during digitization. A few of the units such as the alluvium and talus units were easy to see in the image; however, other units such as the covered bedrock, bedrock, and soil units were more difficult to determine as there were no clear boundaries present and they had the tendency to gradationally blend into each other. Another problem encountered with the image was that some areas of distortion were found in the images taken from the Google Earth™ (Figure 15). For these areas, the image was rechecked by changing the image orientation directly in Google Earth™ in order to facilitate the digitization. Resolution of the composite image also posed some problems in that it was difficult to zoom in close enough to accurately digitized a few of the unit boundaries. Google Earth™ was also rechecked in these instances.

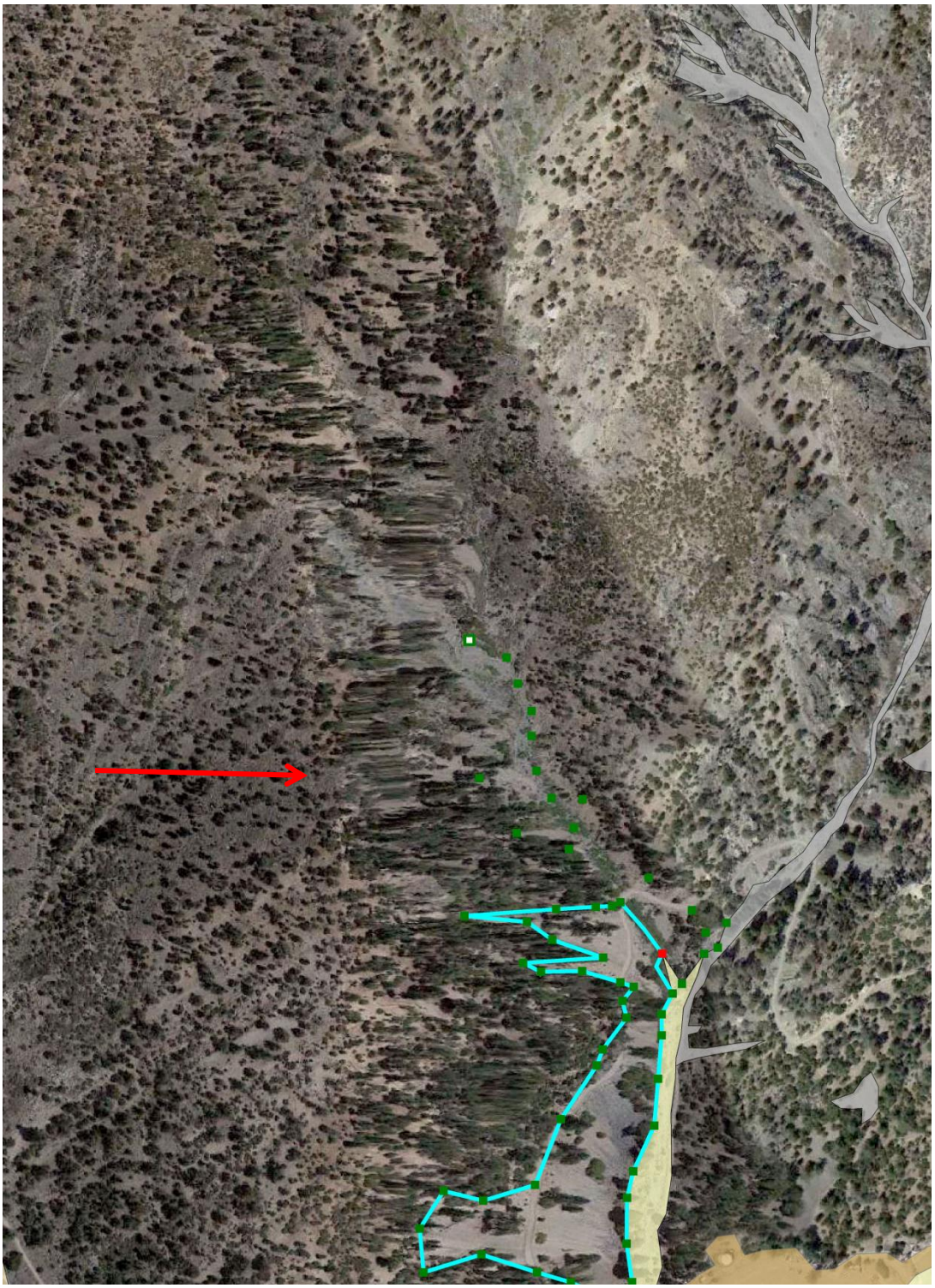

Figure 15. Image during digitization with distortion visible next to the talus unit being digitized. Trees show warping along with the underlying rock/soil unit.

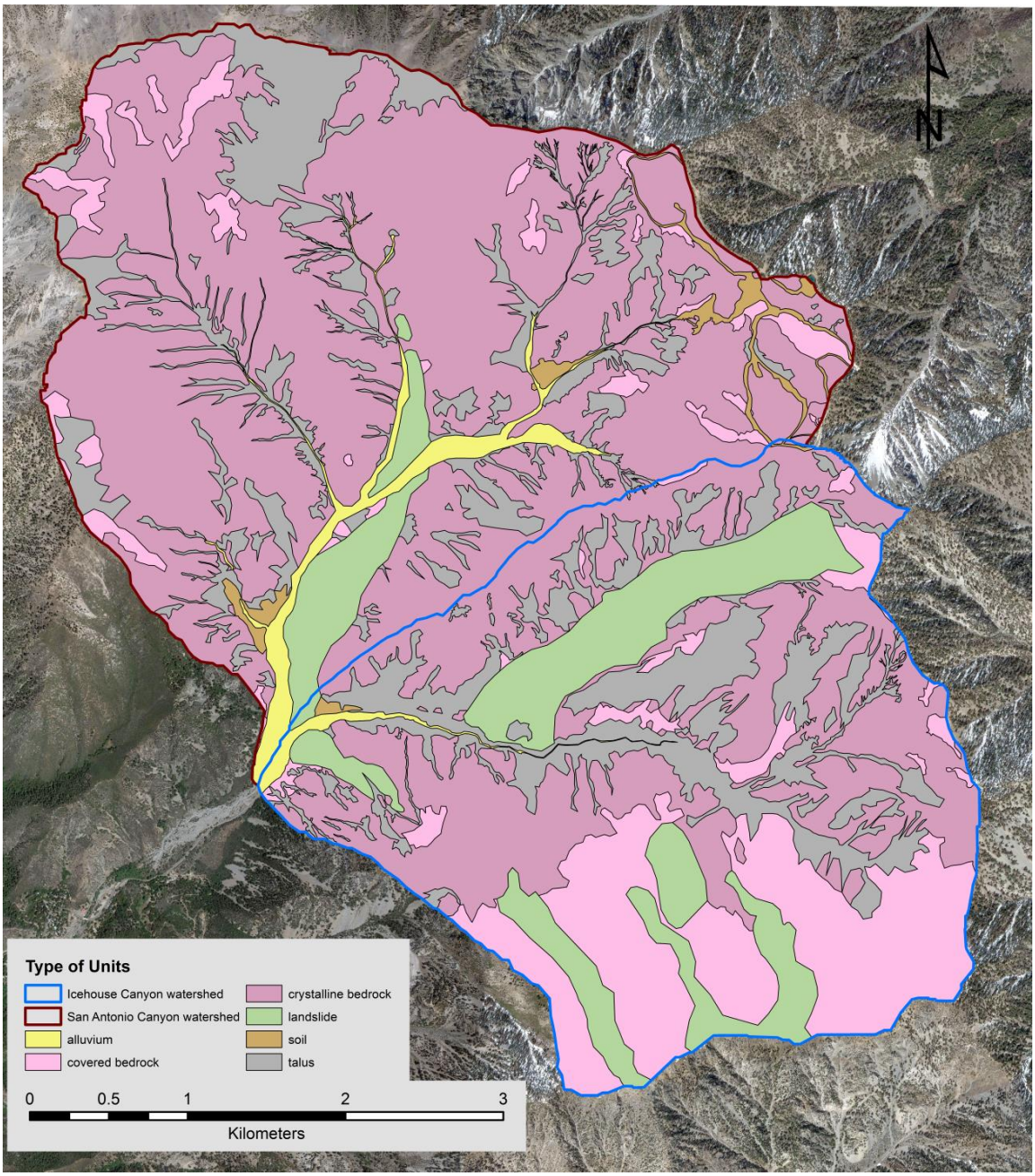

Figure 16. Map of the rock and soil units within the canyons. Landsat image data; Google and the Google logo are registered trademarks of Google Inc., used with permission. Base composite image used is the same as in Figure 11.

Vegetation Analysis

Vegetation units were developed based on the predominant vegetation type present and the habitat in which they are found. California has many distinctive, well characterized habitats that are based on various factors such as climate, elevation, and spatial location (Rundel and Gustafson, 2005). These plant communities typically have a least one dominant plant type that represent the habitat, although because of the Mediterranean climate, other plants can intermingle making it difficult in some cases to determine the predominant plant type (Dole and Rose, 1996). These communities are then given an overall community name such is the case with chaparral which is composed of a wide variety of different, drought tolerant plants. Location may also play a role in some plant communities such as riparian scrub plants. These are typically found in and around alluvial floodplains and consist of drought-deciduous plants that are adapted to porous, low fertility substrates along with periodic flooding (Hanes et al., 1989). My vegetation units were developed to reflect these different habitats. Eight vegetation units and one no vegetation unit were developed for the map (Figure 17). Table 2 shows a detailed list of plants seen in each habitat during field checks that were conducted at various times throughout the past year.

The watershed boundaries were again imported from the Nourse map in order to maintain consistency in the areas digitized. The problems encountered during the vegetation digitization were the same as those encountered during the rock and soil map digitization. Resolution, warping, and boundary problems were rechecked in Google Earth™ during digitization sessions.

A summary table (Table 3) shows the comparison values for the Dibblee, Nourse, and the Google Earth™ rock/soil and vegetation maps. The bedrock unit is the predominant unit in all three maps with San Antonio Canyon consistently higher in the amounts of exposed bedrock than Icehouse Canyon. Other units in San Antonio Canyon and Icehouse Canyon have an overall similar pattern for the proportions of talus vs. alluvium vs. landslide material. However, the actual areas vary widely between the three maps.

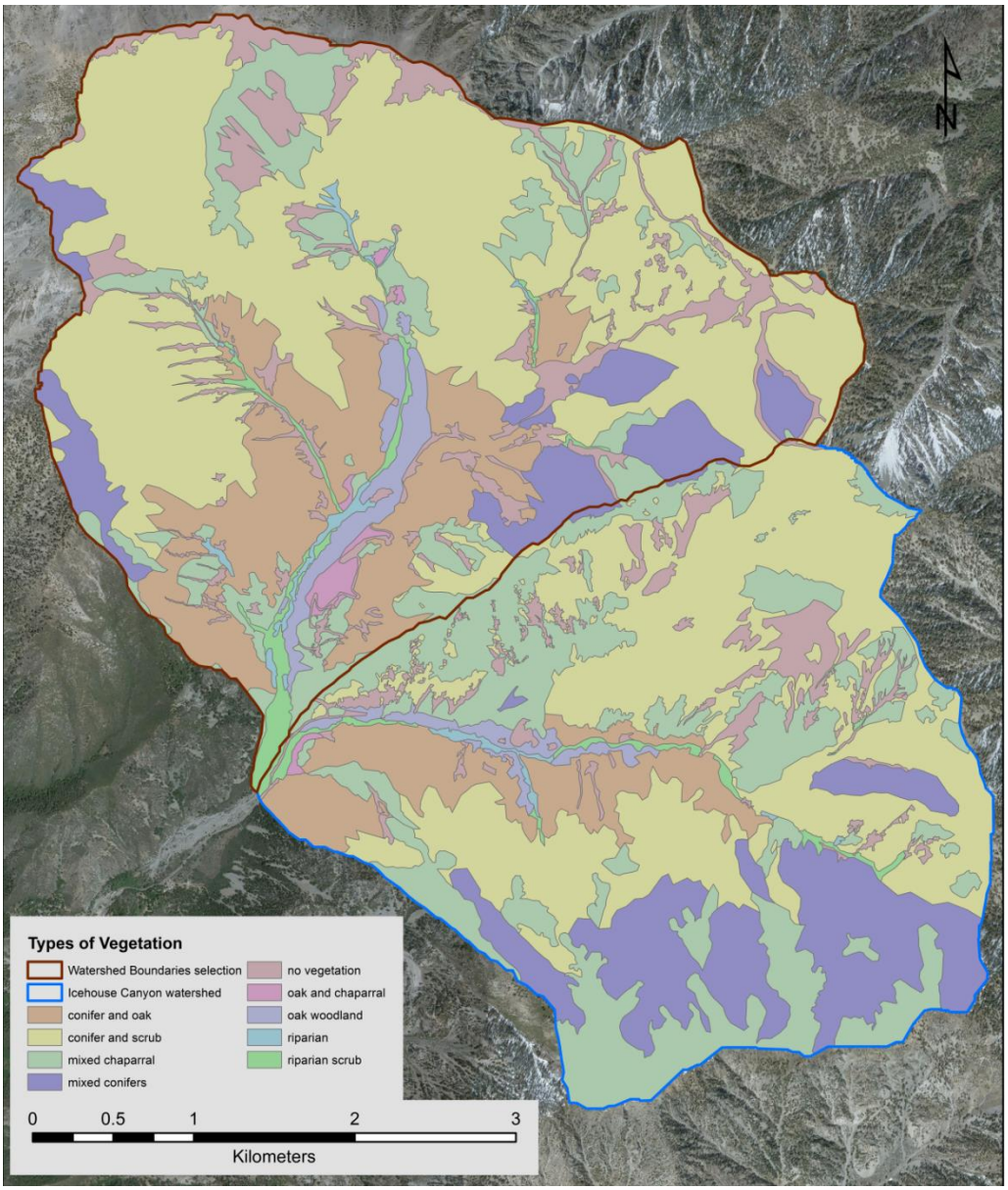

Figure 17. Map of the vegetation units within the canyons. Landsat image data. Base composite image used is the same as in Figure 11.

TABLE 3. COMPARISON DATA FOR DIGITIZED MAP AREAS

Map Units	SAC Area (sq. km)	SAC Percent (%)	IHC Area (sq. km)	IHC Percent (%)
Dibblee				
bedrock (B)	12.34	87.62	8.87	74.56
alluvium (Qal)	0.27	1.90	0.58	4.85
landslide (Qls)	0.57	4.04	1.86	15.61
talus (Qtal)	0.91	6.44	0.59	4.98
Nourse				
bedrock (B)	8.43	59.86	6.16	51.74
alluvium (Qal)	0.59	4.21	0.08	0.66
landslide (Qls)	1.39	9.88	2.25	18.89
talus (Qtal)	3.67	26.05	3.41	28.70
Google Earth- Rock Map				
bedrock (B)	9.69	68.80	4.48	37.64
alluvium (Qal)	0.43	3.08	0.09	0.76
landslide (Qls)	0.57	4.04	1.99	16.77
talus (Qtal)	2.46	17.45	2.31	19.39
covered bedrock (CB)	0.67	4.76	3.01	25.26
soil	0.26	1.87	0.02	0.18
Google Earth- Vegetation Map				
conifer and oak	2.26	16.05	1.13	9.52
conifer and scrub	6.77	48.08	4.46	37.50
mixed chaparral	1.70	12.07	3.23	27.15
mixed conifers	1.14	8.09	1.99	16.69
oak and chaparral	1.43	10.12	0.71	6.00
riparian	0.10	0.70	0.02	0.14
riparian scrub	0.36	2.52	0.18	1.54
oak woodland	0.11	0.76	0.04	0.37
no vegetation	0.23	1.60	0.13	1.08

Digital Elevation Model (DEM) Analysis of Aspect, Slope, Hill Shade, and Insolation

All maps derived from the DEM were processed using the Geoprocessing tools available in ArcMap. The tools used are located in the ArcToolbox under the Spatial Analyst surface tool and contain various functions that can be performed including aspect, hillshade, contour, and slope. Some of these tools require the user to enter in specific information such as azimuth, altitude, and a correction factor called a z-factor which is used to adjust the elevation units to match the horizontal x,y coordinate units and is dependent upon the latitude of the study area. Applying a z-factor is especially important when input raster has a decimal degree coordinate system. Improperly set z-factors will result in an incorrect map. A z-factor of 0.00001069 was calculated for the latitude of 34.27° by first converting the degree value to radians then using the following equation,

$$\text{z-factor} = 1.0 / (113200 * \cos(\text{latitude in radians})) \quad (1)$$

and was used for all geoprocessing that requires a z-factor.

The insolation analysis presented in the last part of this chapter is especially powerful because it effectively calculates spatial distribution of solar energy influx at various times of the year. Insolation, in concert with vegetation coverages, are expected to be important controls on evapotranspiration rate.

Aspect Analysis

Aspect maps were made in ArcMap to determine the direction of the slope faces in both of the watersheds. A DEM raster data set was used for the analysis and the change in slope was determined by the maximum change in direction from one raster cell to the next with the output information in degrees of slope angle. Figure 18 shows the result of the analysis for upper San Antonio Canyon. Slope faces were determined in 30 degree increments for both watersheds. A histogram was prepared for the slope data to quantify the proportion of slope areas that face in a particular direction (Figure 19). This derivative plot shows that there is a distinct south-southwest facing trend in Upper San Antonio Canyon.

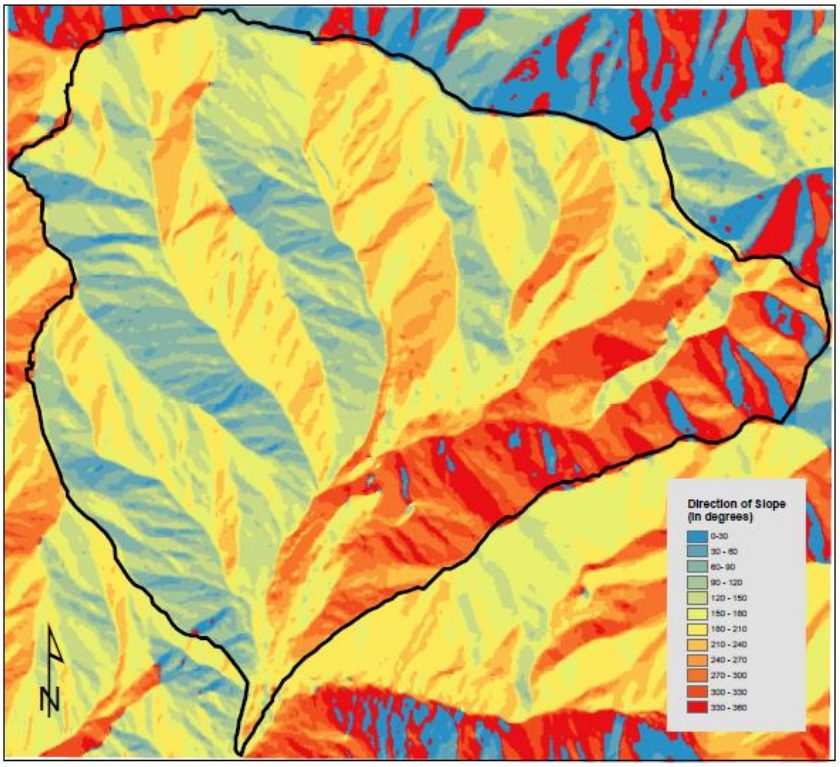

Figure 18. Aspect map of upper San Antonio Canyon. The map shows the direction of slope with color boundaries set at increments of 30 degrees azimuth.

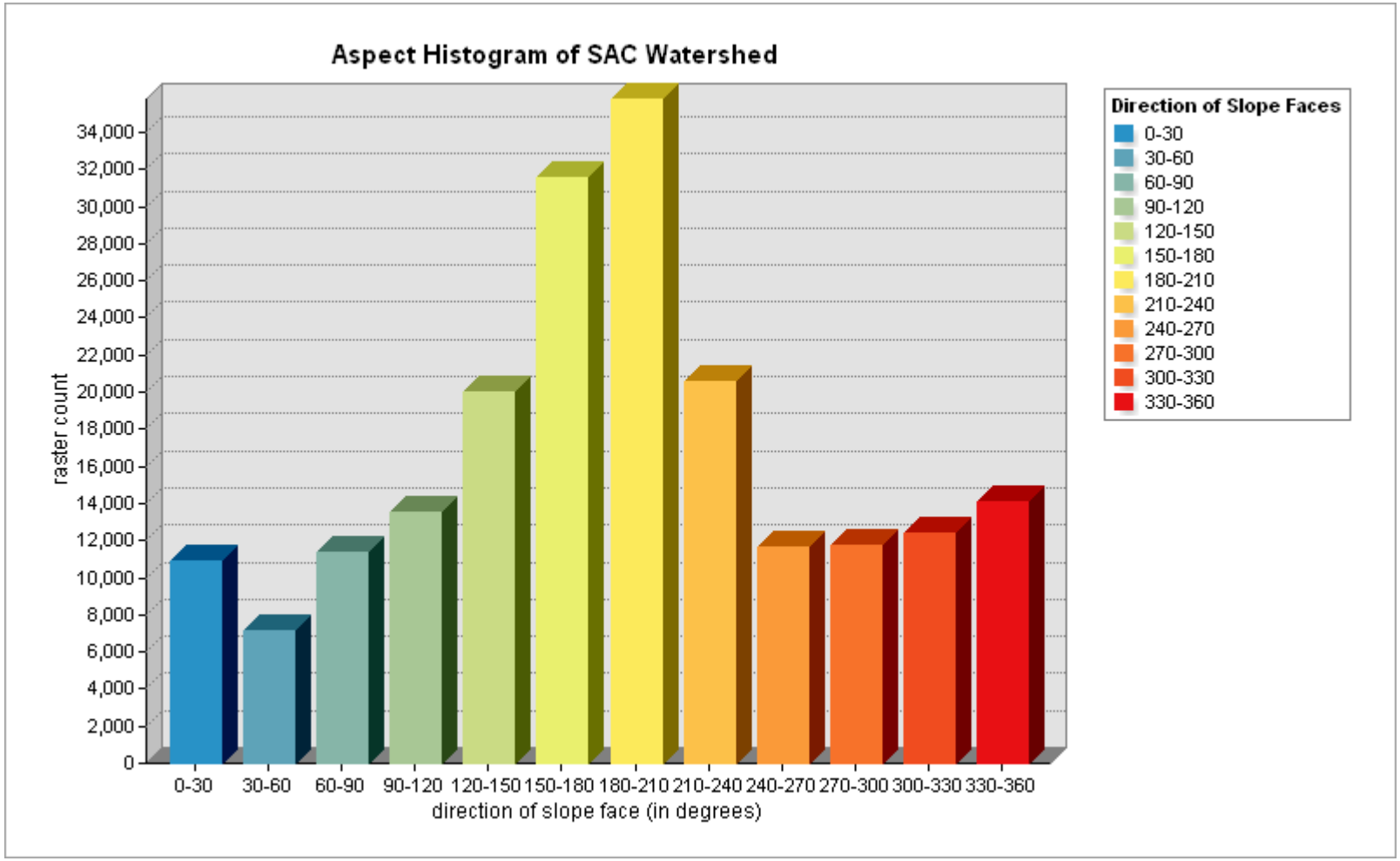

Figure 19. Histogram for San Antonio Canyon slope aspect data. The histogram clearly shows a distinct south-southwest facing trend.

This trend suggests that San Antonio Canyon which is more open and faces the sun should have a solar insolation influx higher than Icehouse Canyon. Differences in vegetation should also be reflected with this trend. The vegetation for upper San Antonio watershed should be those types of plants that can tolerate less water i.e. chaparral plants or have the ability to access deeper groundwater reserves such as the mixed conifers *(Pinus sp.)*.

The aspect map for Icehouse Canyon (Figure 20) shows a much different pattern than San Antonio. Icehouse Canyon has distinct north and south facing trends with at least half of the watershed facing northwards (Figure 21). This suggests that there will be less solar insolation received throughout the year which in turn should affect the types of vegetation seen. Vegetation located in Icehouse Canyon is dependent on the direction and amounts of sun received canyon. Vegetation on the north facing slopes should be thicker and require less water than the vegetation on the south facing slopes due to the drier conditions. Evidence for this is found in the types of vegetation mapped within the canyon. Large oaks *(Quercus sp.)*, which typically have higher water requirements than chaparral, were found on the south side of the canyon but few were seen on the north side except for those very near the Icehouse Creek in the oak woodlands. Chaparral was only seen on the north side of the canyon on slopes that have a more southerly facing direction. The minimums in the histogram (Figure 21) also indicate that relatively small areas of the slopes face east or west. This is a direct manifestation of the east-west trend of Icehouse Canyon.

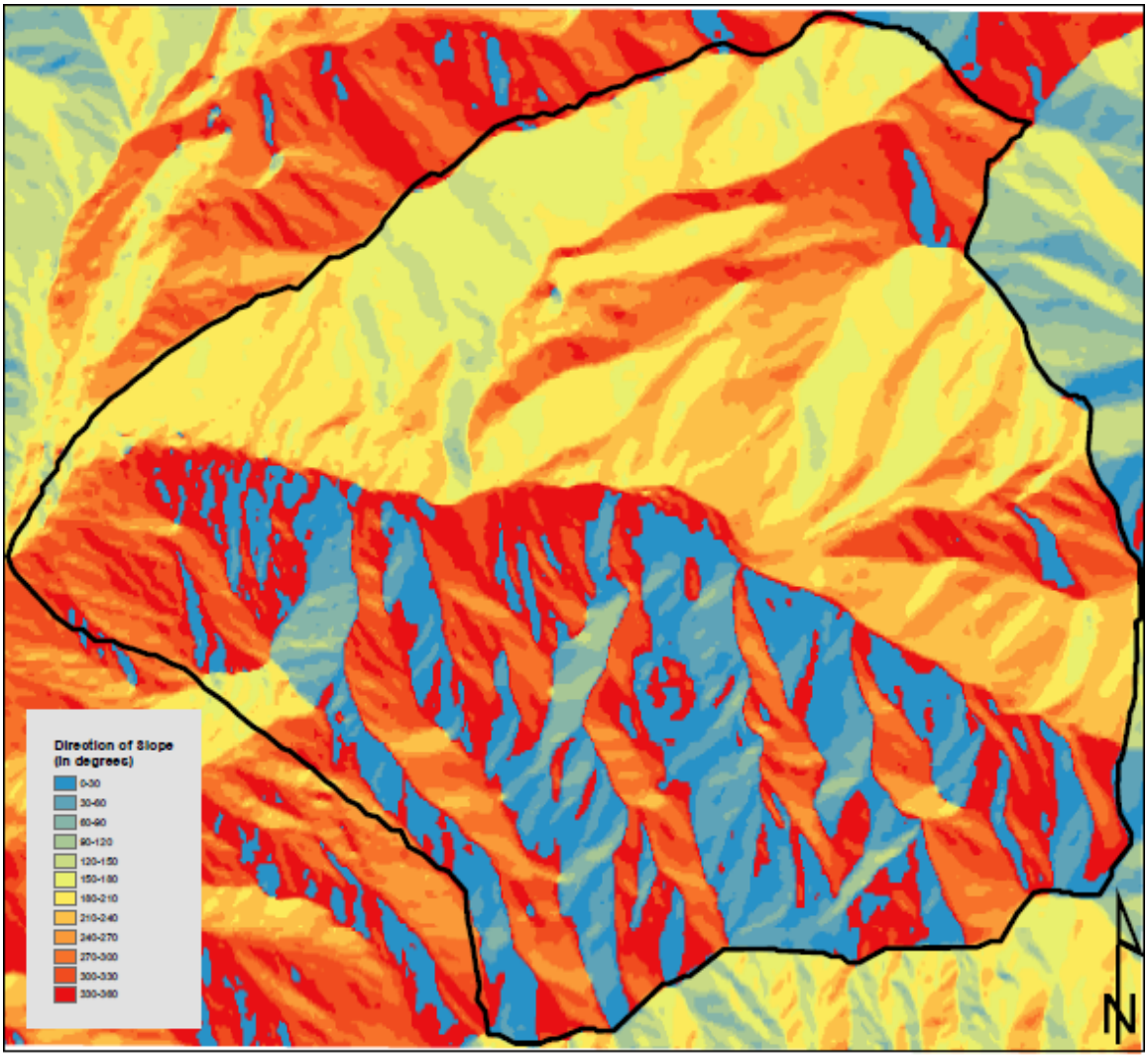

Figure 20. Aspect map of Icehouse Canyon, This map shows the direction of slope.

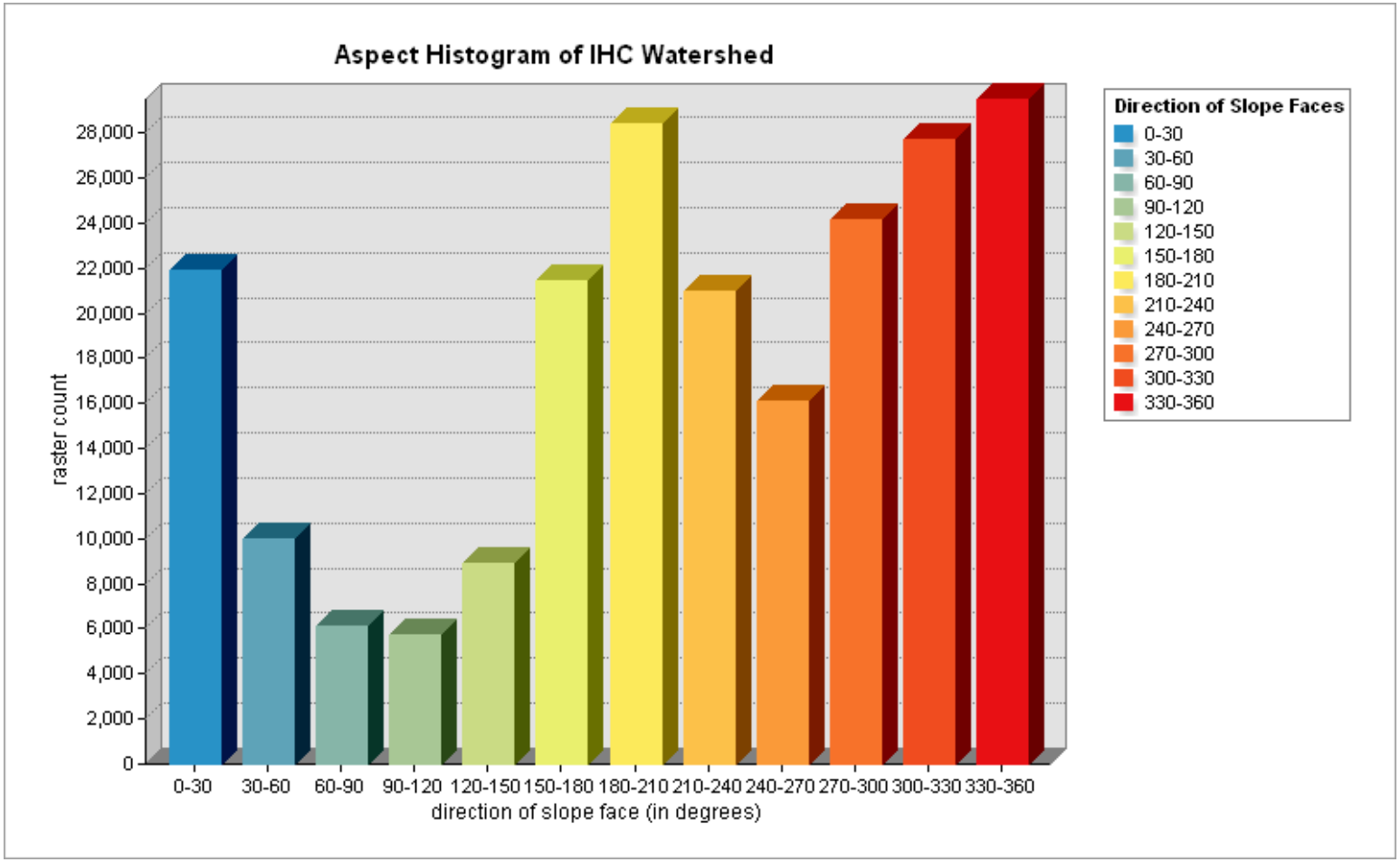

Figure 21. Histogram for Icehouse Canyon. The histogram shows a predominant north-south facing direction for most of the slope faces in the canyon. Note the minimums occur along easterly and westerly azimuths.

Slope Analysis

Slope is determined from the DEM raster data set and is the measure of steepness found within the canyons. ArcMap calculates the maximum change in elevation for each raster cell and its surrounding cells by using basic trigonometric functions to determine the slope angle in degrees. A z-factor of 0.00001069 was applied to the data. The derived slope is shown in Figure 22 for upper San Antonio Canyon. The green colors represent gentler slope angles while changing towards red for the higher slope angles. It is somewhat difficult to determine the actual predominant slope angle from the map, but some of the red areas approach near vertical cliffs. A histogram (Figure 23) was prepared that more clearly shows the actual slope variations and their relative proportions. A second slope map and histogram were also prepared of Icehouse Canyon for comparison and are shown in Figures 24 and 25. By comparing the two histograms, both canyons are fairly similar in topography with predominant slope values ranging from 35 to 40 degrees. In Icehouse Canyon, the steepest slopes are on the north face of Ontario Ridge and the south face of the south summit of Telegraph Peak.

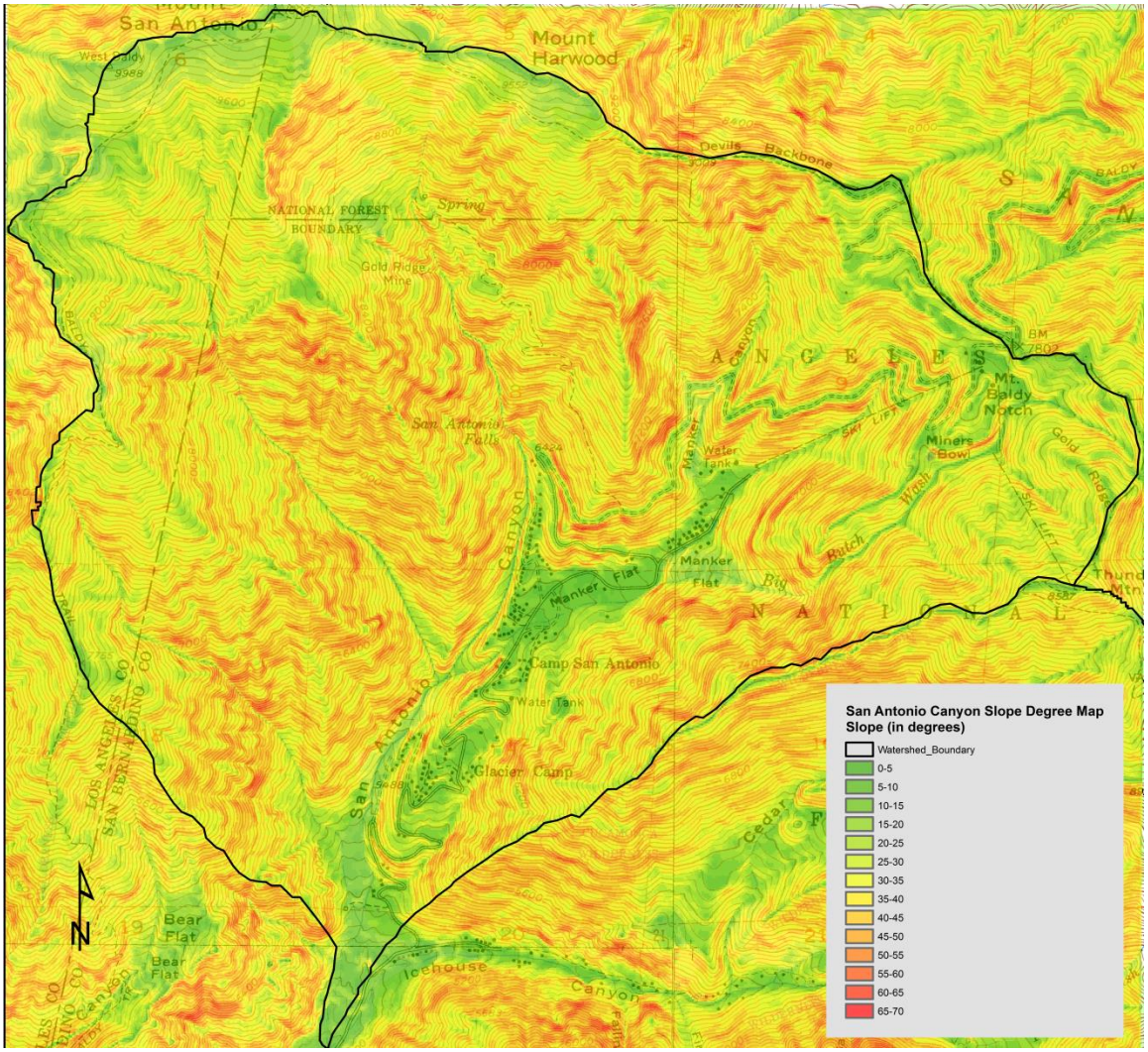

Figure 22. Slope map for San Antonio Canyon. The map shows the slope angles or steepness.

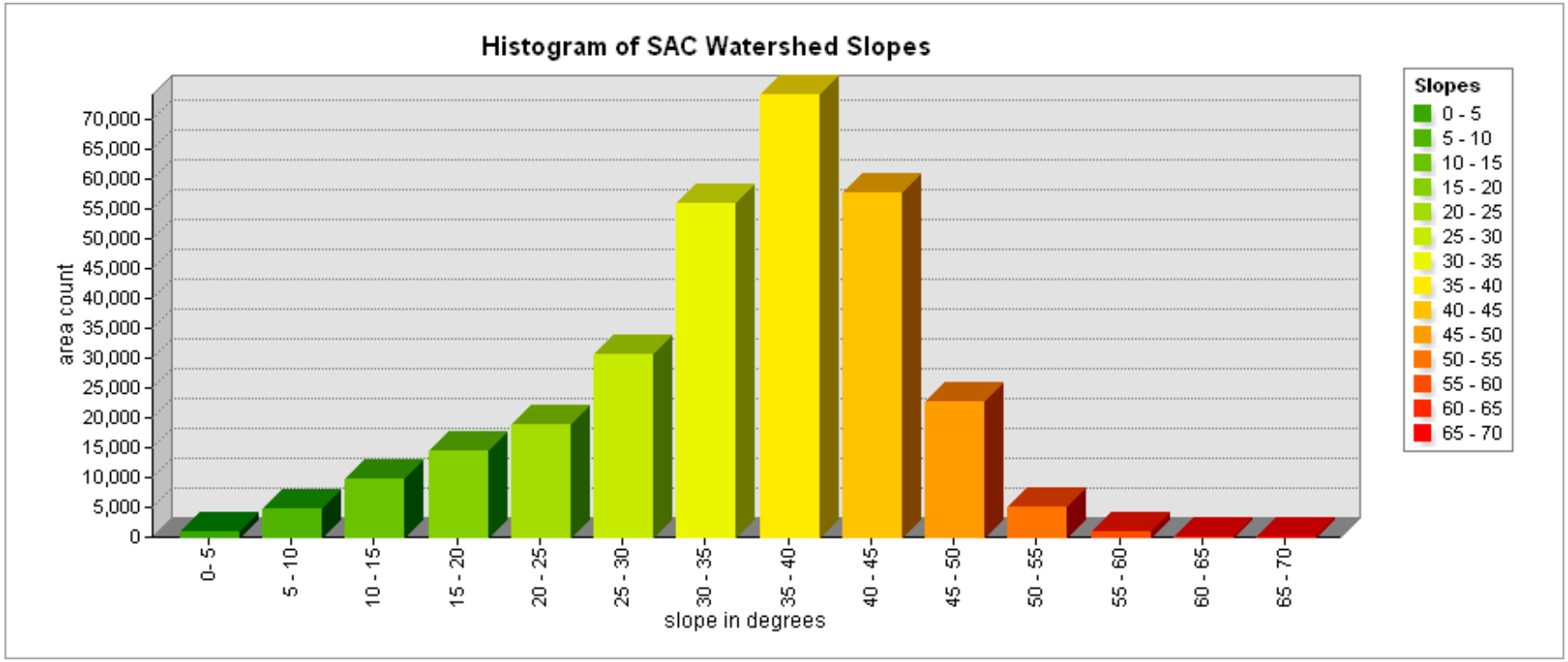

Figure 23. Histogram showing a predominant slope angle between 35 to 40 degrees. The mean slope angle is 34 degrees.

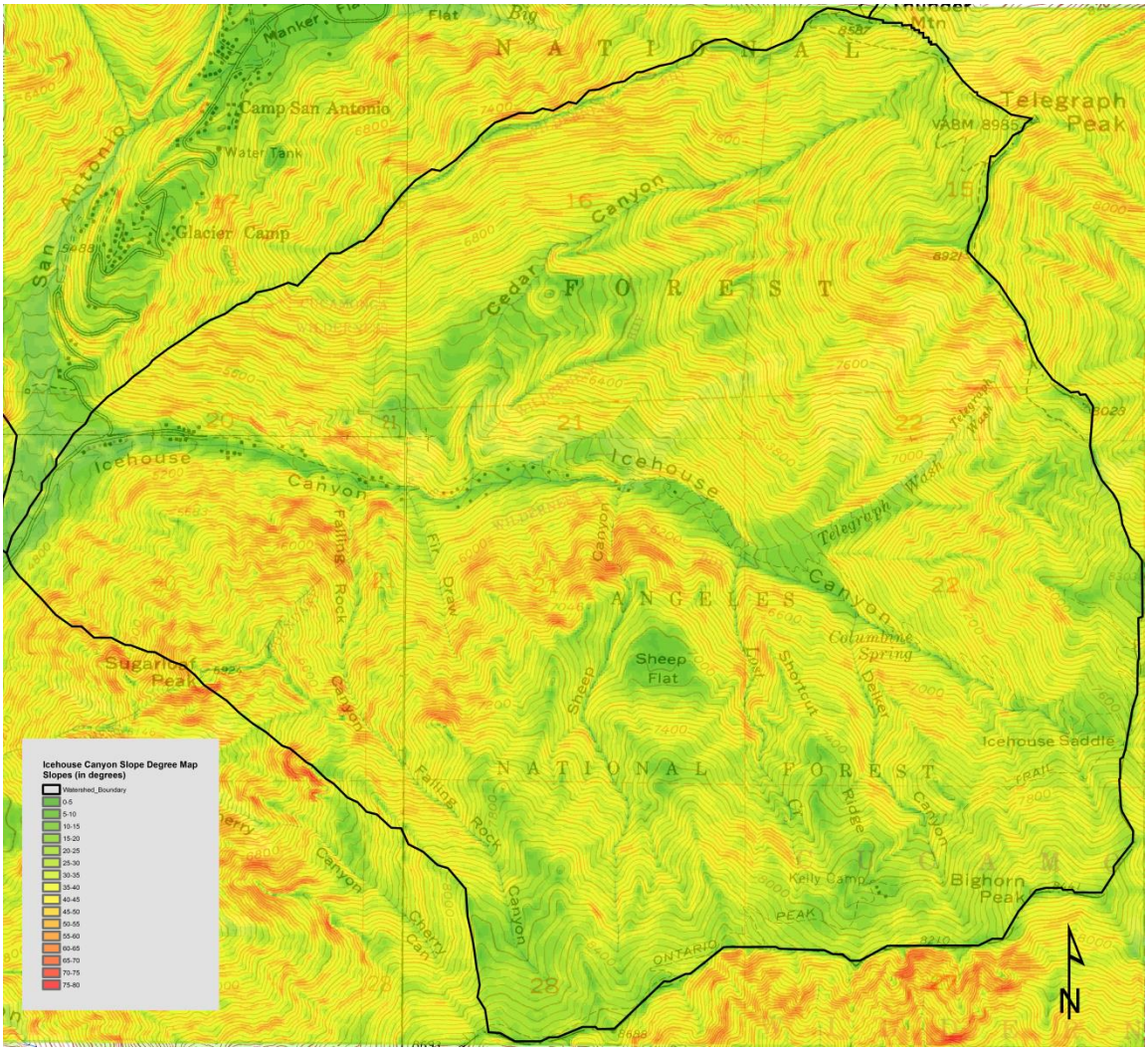

Figure 24. Slope map for Icehouse Canyon showing the slope angles or steepness.

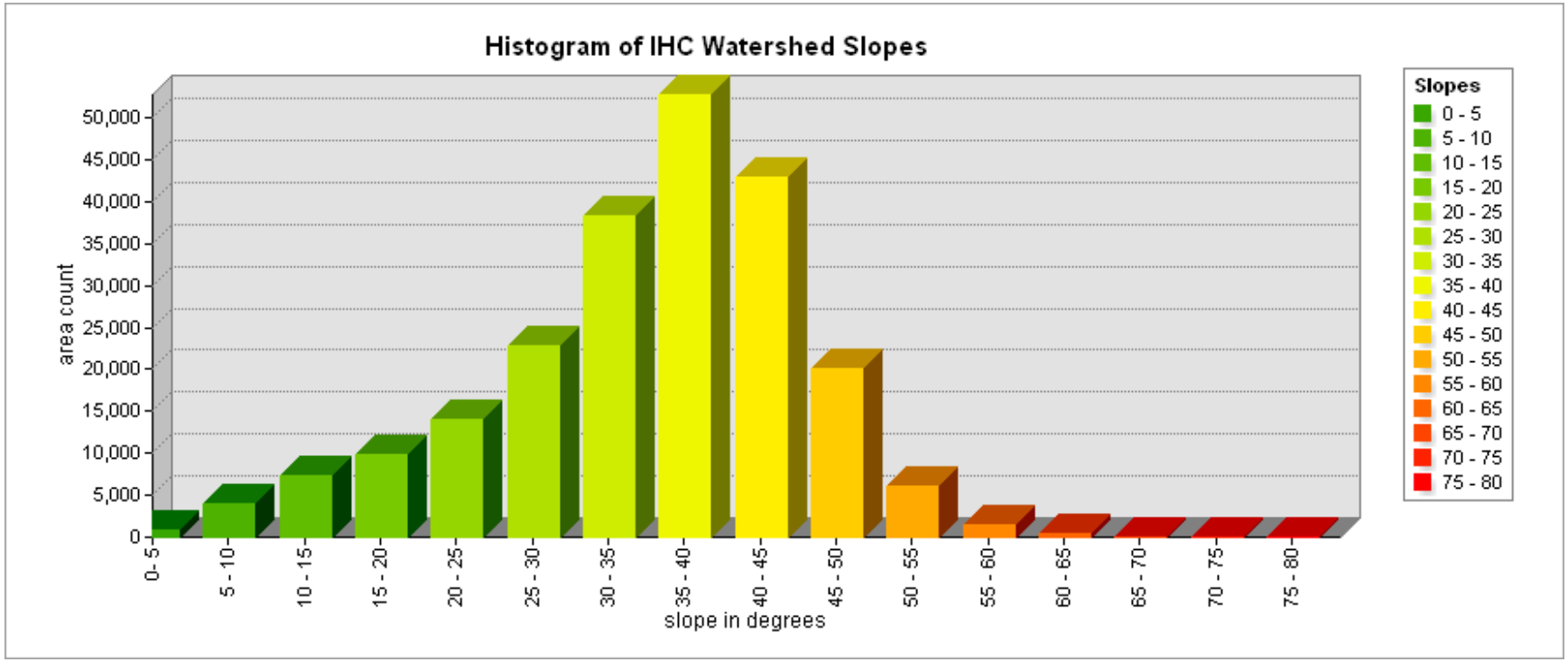

Figure 25. Histogram showing a predominant slope angle between 35 to 40 degrees. The mean slope angle is 34 degrees.

Hill Shade Analysis

Hill shade maps were made for the four 2015 seasons : the spring equinox, the summer solstice, the fall equinox, and the winter solstice using the hillshade tool in ArcMap (Figures 27-34). Hill shade maps are shaded relief maps that can be draped over a topographic map creating a three dimensional effect that helps to bring out topographical differences. Azimuth and altitude settings can be changed from the preset default settings to reflect the actual sun's position in the horizon for any date (Figure 26) as long as the angles are known for those dates. The sun's positions were determined for the different seasons and are shown in Table 4. These values were used to model both the hill shade and solar insolation maps. Both the spring and fall equinoxes have almost the same sun elevation and direction resulting in maps that appear essentially identical.

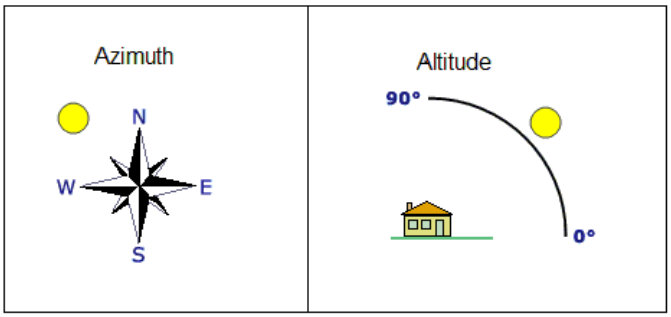

Figure 26. Diagram of azimuth and altitude. (Adapted from ESRI.com).

TABLE 4. PREDICTED SEASONAL SOLAR DATA AT NOON

Date	Season	Azimuth	Altitude
3/20/2015	spring equinox	180.85°	55.67°
6/21/2015	summer solstice	189.18°	79.02°
9/23/2015	fall equinox	187.49°	55.29°
12/21/2015	winter solstice	183.06°	32.21°

Note: All values were determined at noon; adjusted for daylight savings as needed. This is why the azimuth differs between summer and winter and between fall and spring.

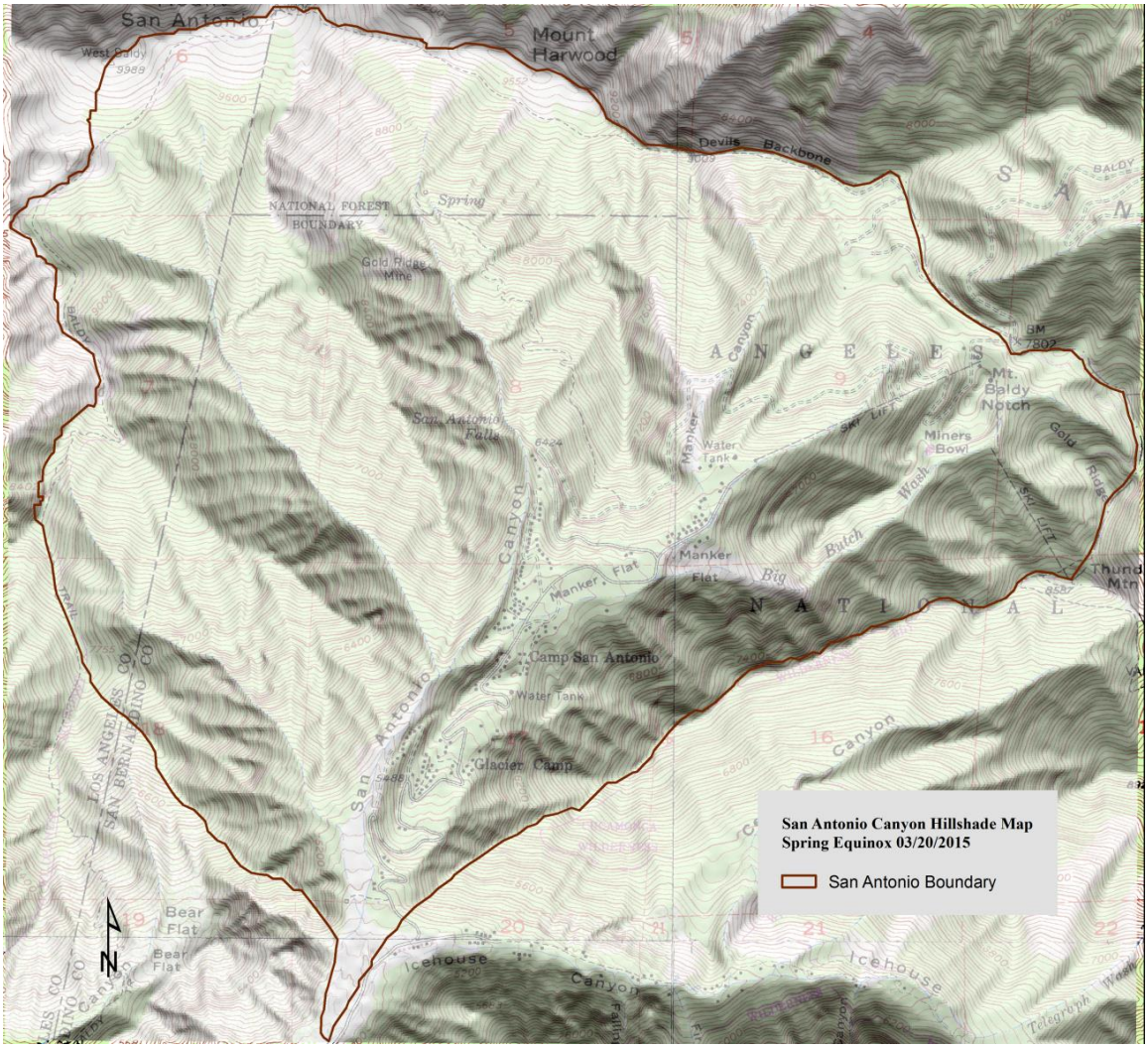

Figure 27. Hill shade map of San Antonio Canyon-spring equinox at noon. Hill shade raster data is draped over USGS DRG topographic map rendering a three dimensional effect.

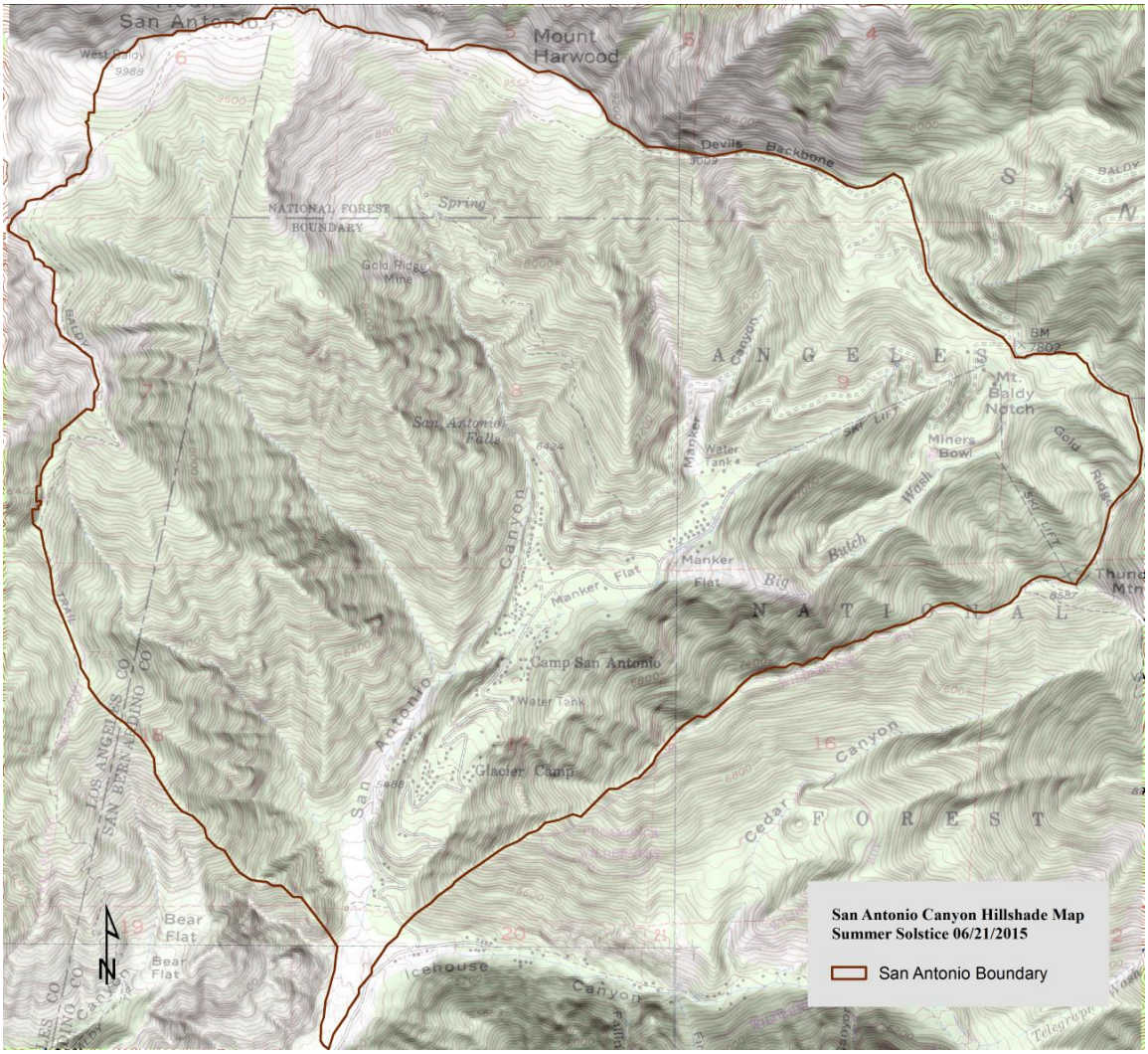

Figure 28. Hill shade map for San Antonio Canyon-summer solstice at noon.

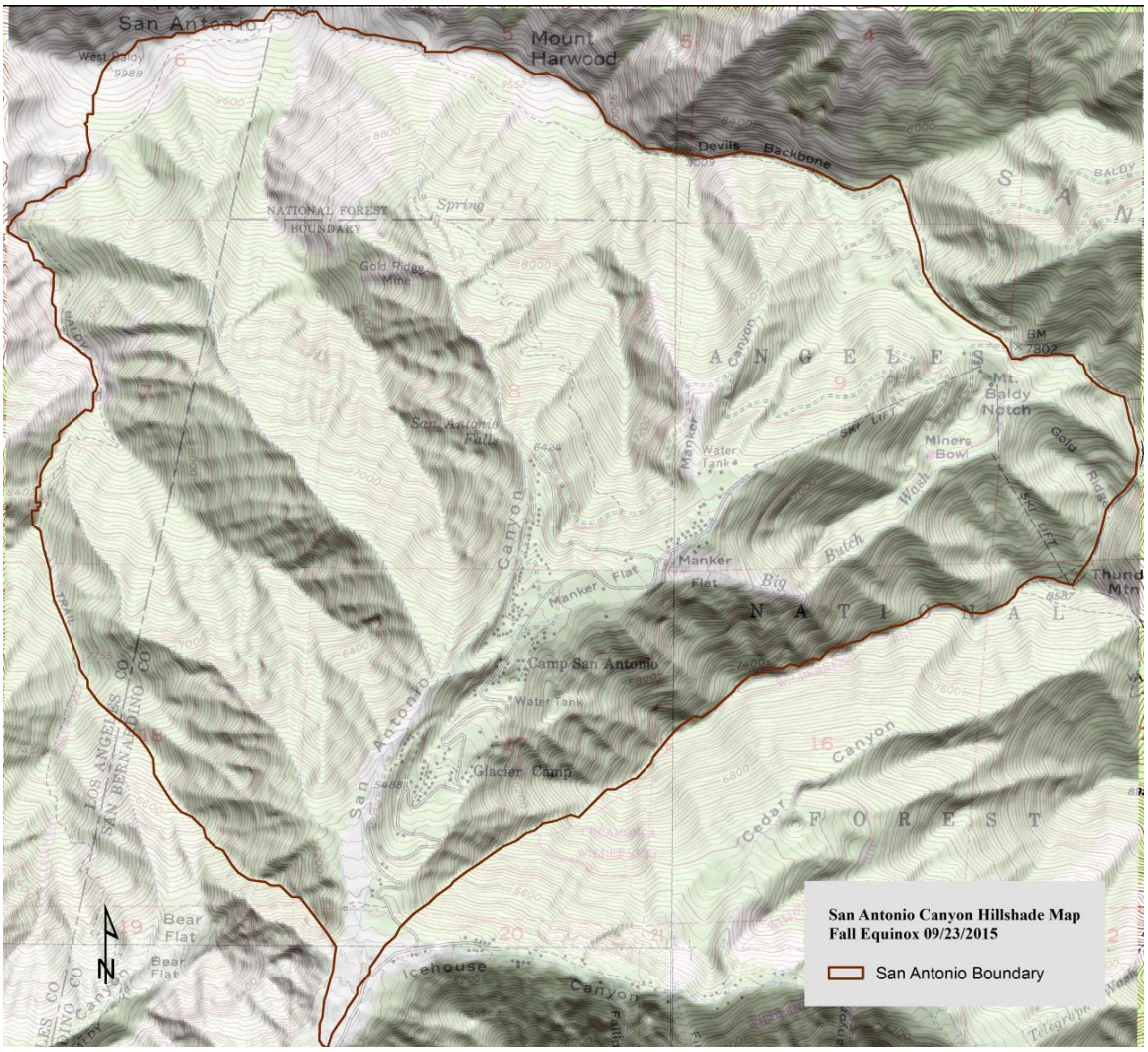

Figure 29. Hill shade map for San Antonio Canyon-fall equinox at noon.

Figure 30. Hill shade map for San Antonio Canyon-winter solstice at noon.

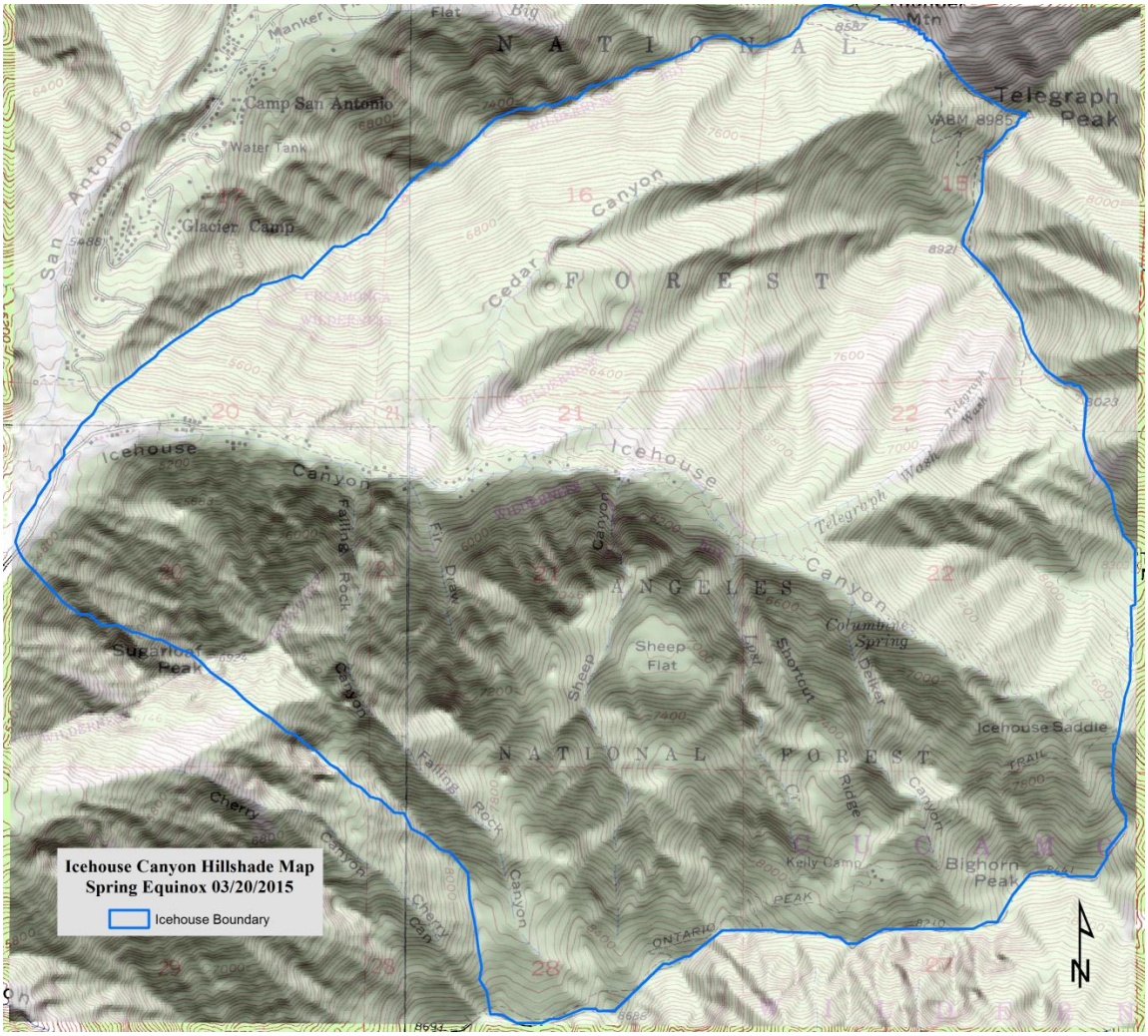

Figure 31. Hill shade map for Icehouse Canyon-spring equinox at noon.

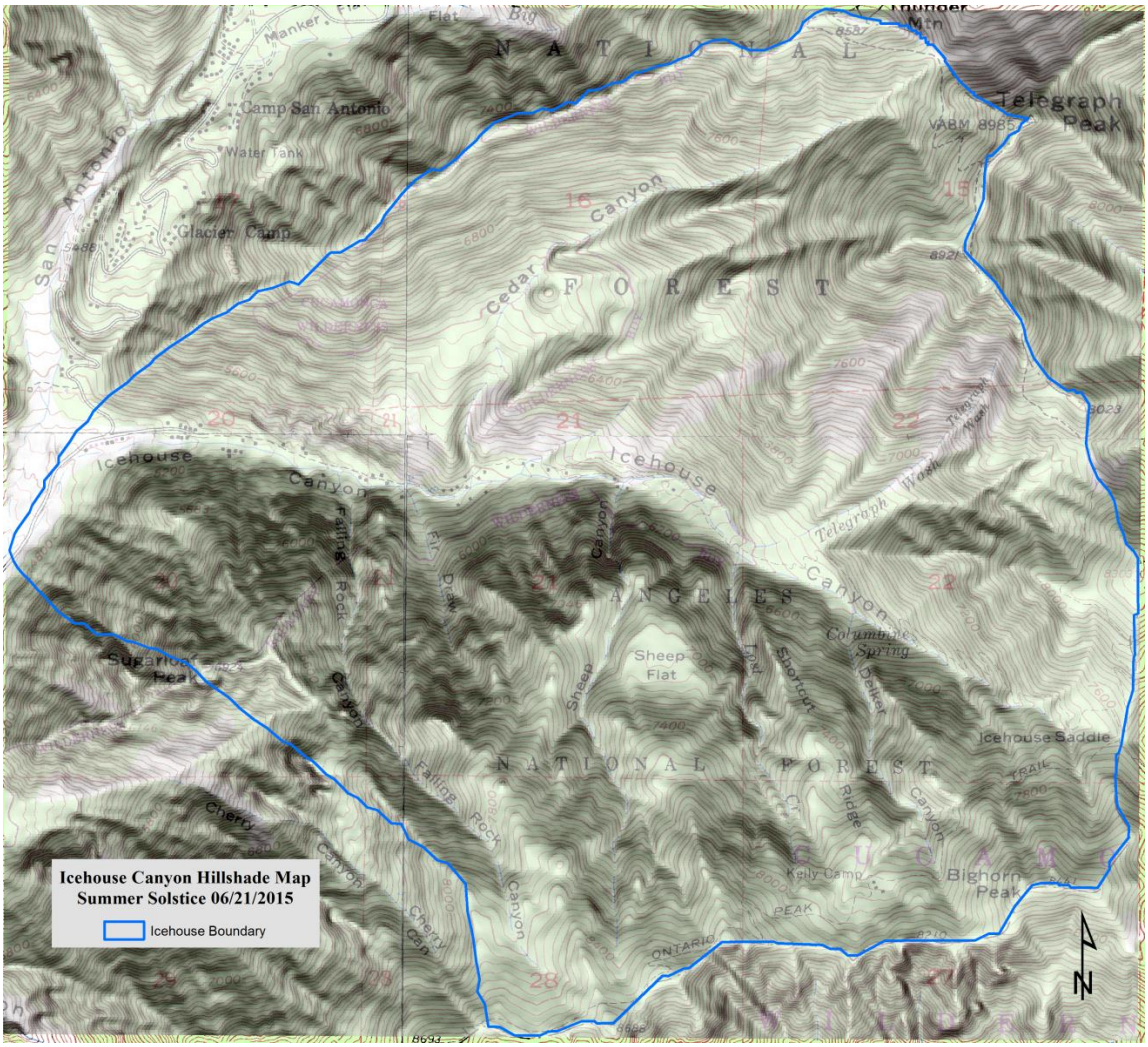

Figure 32. Hillshade map for Icehouse Canyon-summer solstice at noon. Note how the Cedar Canyon and Sheep Flat landslides become much more prominent with the relief added.

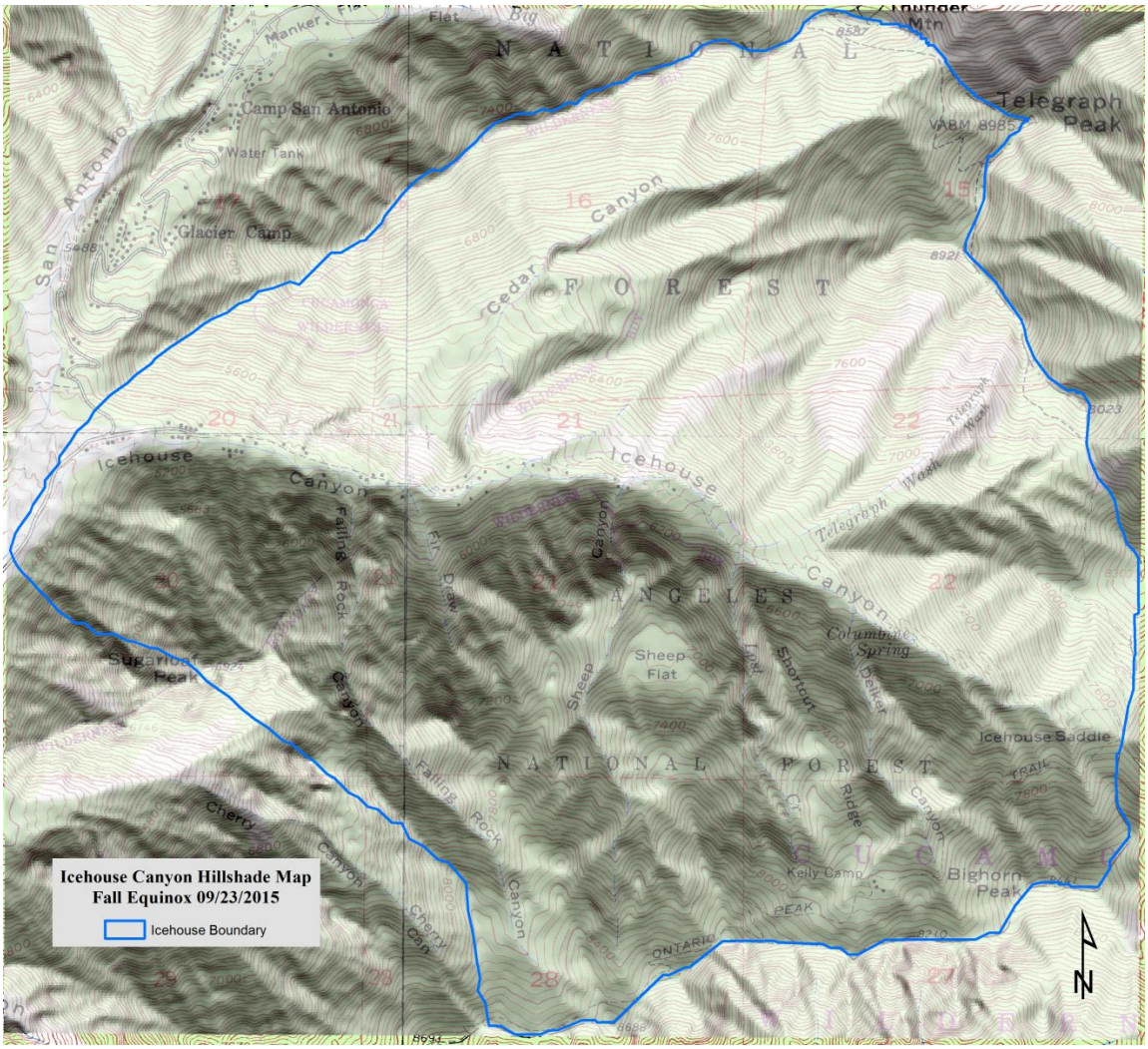

Figure 33. Hill shade map for Icehouse Canyon-fall equinox at noon.

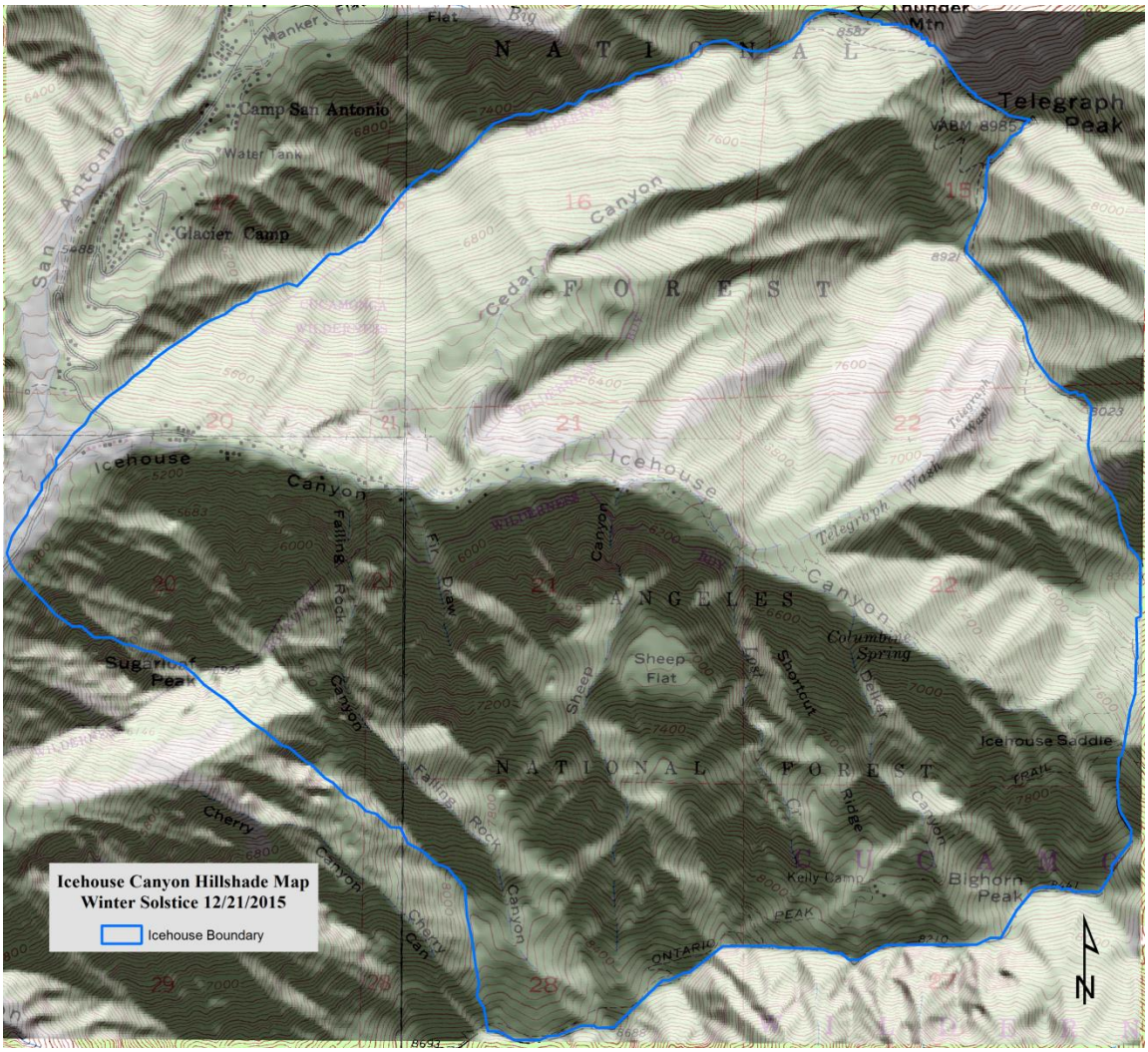

Figure 34.. Hill shade map for Icehouse Canyon-winter solstice at noon. Note the entire southern portion of the watershed is in deep shade.

These maps were developed to show the relative amounts of shade present at noon throughout the watersheds and to illustrate the topography found in the canyons. This shading can be correlated with lower temperatures and lower evaporation rates. To some degree there will be even more shadows in these areas during morning and afternoon, although direction of slope facing is a factor. The hillshade effects are especially dramatic in Icehouse Canyon because most of the slopes face either north or south, directly away from or towards the sun's azimuth at noon.

Solar Insolation Analysis

Determining incoming solar radiation is one of the most important factors in the analysis of the watersheds. Solar insolation amounts are primarily dependent upon the topography of an area (Fu and Rich, 1999). Elevation, slope, aspect, and hill shade all contribute to how solar radiation is received in the two canyons. Other factors such as time of day and sun angle will contribute to the variability of the microclimates seen in both watersheds. The amount of solar radiation received directly affects soil moisture and soil temperatures causing different plant populations to form. Correlation with evapotranspiration rate is also expected.

Solar insolation maps were derived from the DEM raster data using sophisticated tools that enable the amount of radiation (solar energy flux) to be determined over a geographical area for specific time periods. Two types of radiation, direct and diffuse, were calculated then combined by ArcMap to form one insolation map for each of the selected dates. Direct radiation is the measure of . Diffuse radiation is the measurement of . Reflected radiation is not calculated by ArcMap since reflected radiation is only a minor component of the total amount of solar radiation. The ArcMap solar radiation tool calculates the values for an area in units of watt hours per square meter (WH/m^2) for a specified time period with the desired sun angles. Other parameters are inputted before processing the DEM. Results for the four 2015 seasons were calculated using the parameters listed in Table 5. Figures 36-43 show the predicted results of the solar radiation analysis for upper San Antonio and Icehouse Canyons.

When examining the four maps for upper San Antonio Canyon and Icehouse Canyon, the two equinoxes appear identical to each other (Figures 36, 38 and Figures 40, 42 respectively) as expected due to the input values used. Also, length of day and sun's position in the sky are the same for the two equinoxes.

TABLE 5. PARAMETERS FOR SOLAR INSOLATION CALCULATIONS

Parameter	Value	Description
latitude	34.288897	latitude for Mt. San Antonio in decimal degrees
sky_ size	5000	resolution for the calculated sky and sun maps (raster of 5000x 5000 cells)
time_ configuration	TimeWithinDay	one calendar day (date selectable)
day_ interval	14	
hour_ interval	0.5	time interval through the day used to calculate sky sectors
z_factor	0.00001069	correction for geographic coordinate system rasters
slope_ aspect_ input_ type	FROM_DEM	how slope and aspect are derived for analysis
calculation_directions	48	the number of azimuth directions used when calculating the viewshed; higher number are used for complex topography
zenith_divisions	8	the number of divisions used to create sky sectors in the sky map
azimuth_divisions	8	the number of divisions used to create sky sectors in the sky map
diffuse_model_type	UNIFORM_SKY	the incoming diffuse radiation is the same in all sky directions
diffuse_proportion	0.3	the proportion of global normal radiation flux that is diffuse; clear sky conditions
transmittivity	0.5	the fraction of radiation that passes through the atmosphere average over all wavelengths; clear sky conditions

Predicted solar insolation values for the two watersheds are shown in Table 6 with values calculated for a 24 hour period. The maps shown below in Figures 36-43 were plotted to the same color scale for solar insolation values ranging from a low of 290 WH/m^2 to a high value of 8250 WH/m^2. Table 6 seems to imply that the amount of solar radiation received are roughly equivalent; however, this is not the case. The table shows that both watersheds have the similar high and low radiation values for each cell.

Four histograms were prepared for Upper San Antonio Canyon and Icehouse Canyon using the winter and summer solstices which show the actual insolation trends. It is readily apparent that there are differences seen not only for the different solstices but also between the two canyons (Figure 35).

TABLE 6. PREDICTED SEASONAL SOLAR INSOLATION DATA

Date	Season	Minimum (WH/m^2)	Maximum (WH/m^2)
San Antonio Canyon			
3/20/2015	spring equinox	560	6262
6/21/2015	summer solstice	2929	8225
9/23/2015	fall equinox	558	6244
12/21/2015	winter solstice	291	3656
Icehouse Canyon			
3/20/2015	spring equinox	568	6037
6/21/2015	summer solstice	2248	7959
9/23/2015	fall equinox	566	6020
12/21/2015	winter solstice	293	3524

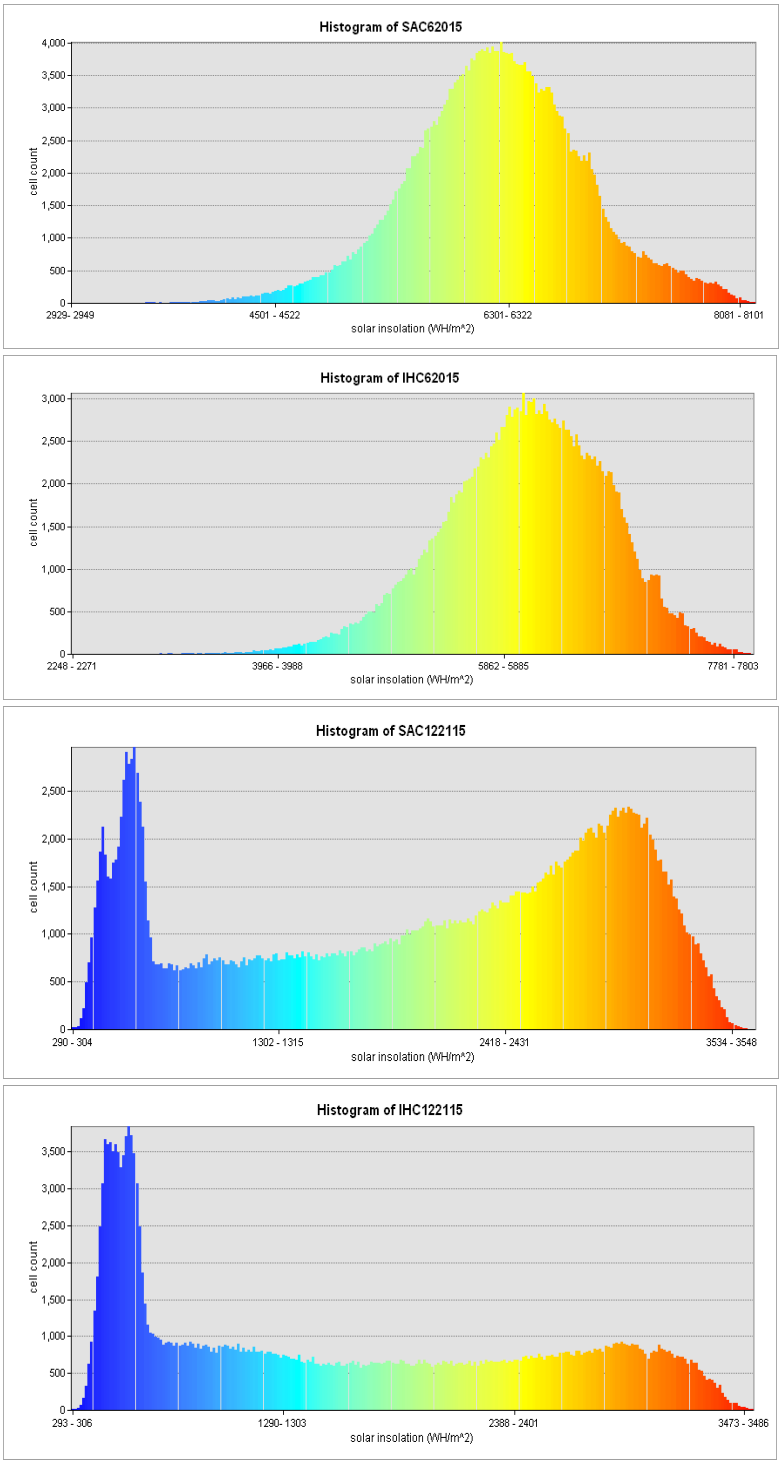

Figure 35. Solar histograms for winter and summer solstices. A) San Antonio Canyon- 06/20/15, B) Icehouse Canyon- 06/20/15, C) San Antonio Canyon- 12/21/15, D) Icehouse Canyon- 12/21/15. Differences can be seen in the distribution patterns of the histograms based on area counts and solar insolation values.

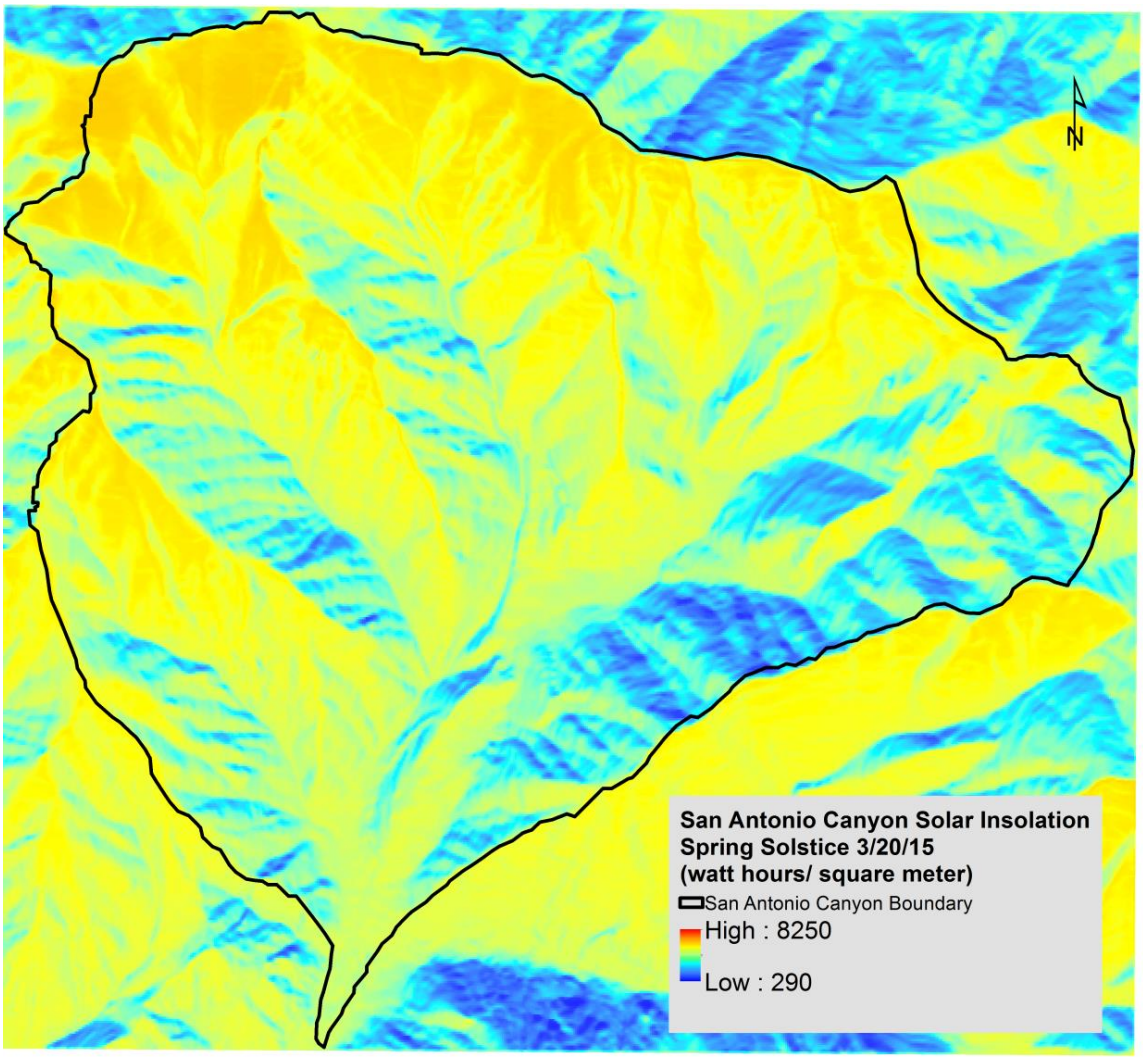

Figure 36. Solar insolation map for San Antonio Canyon-spring equinox. Red are areas of high solar insolation while blue represents areas of low insolation.

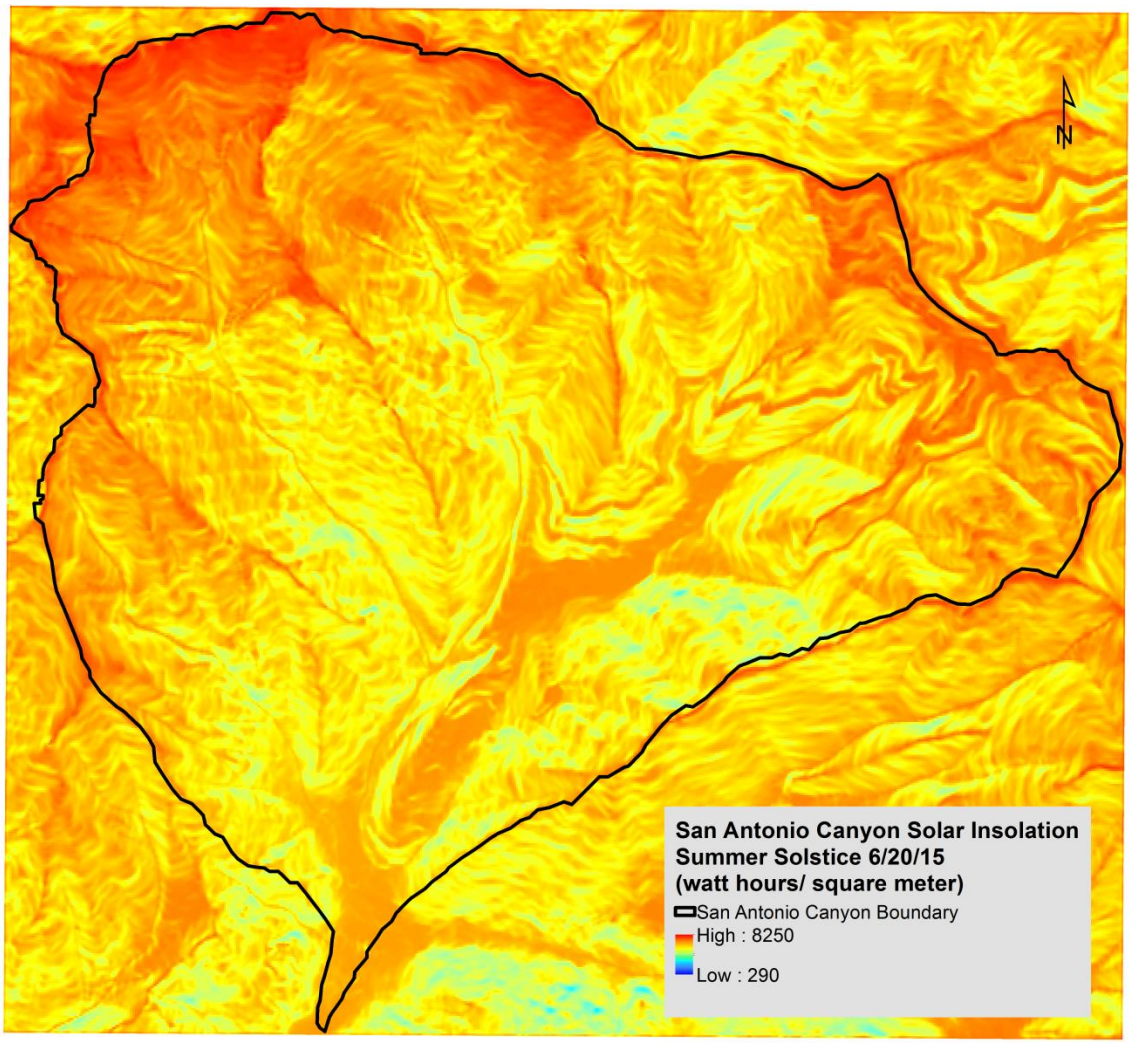

Figure 37. Solar insolation map for San Antonio Canyon-summer solstice.

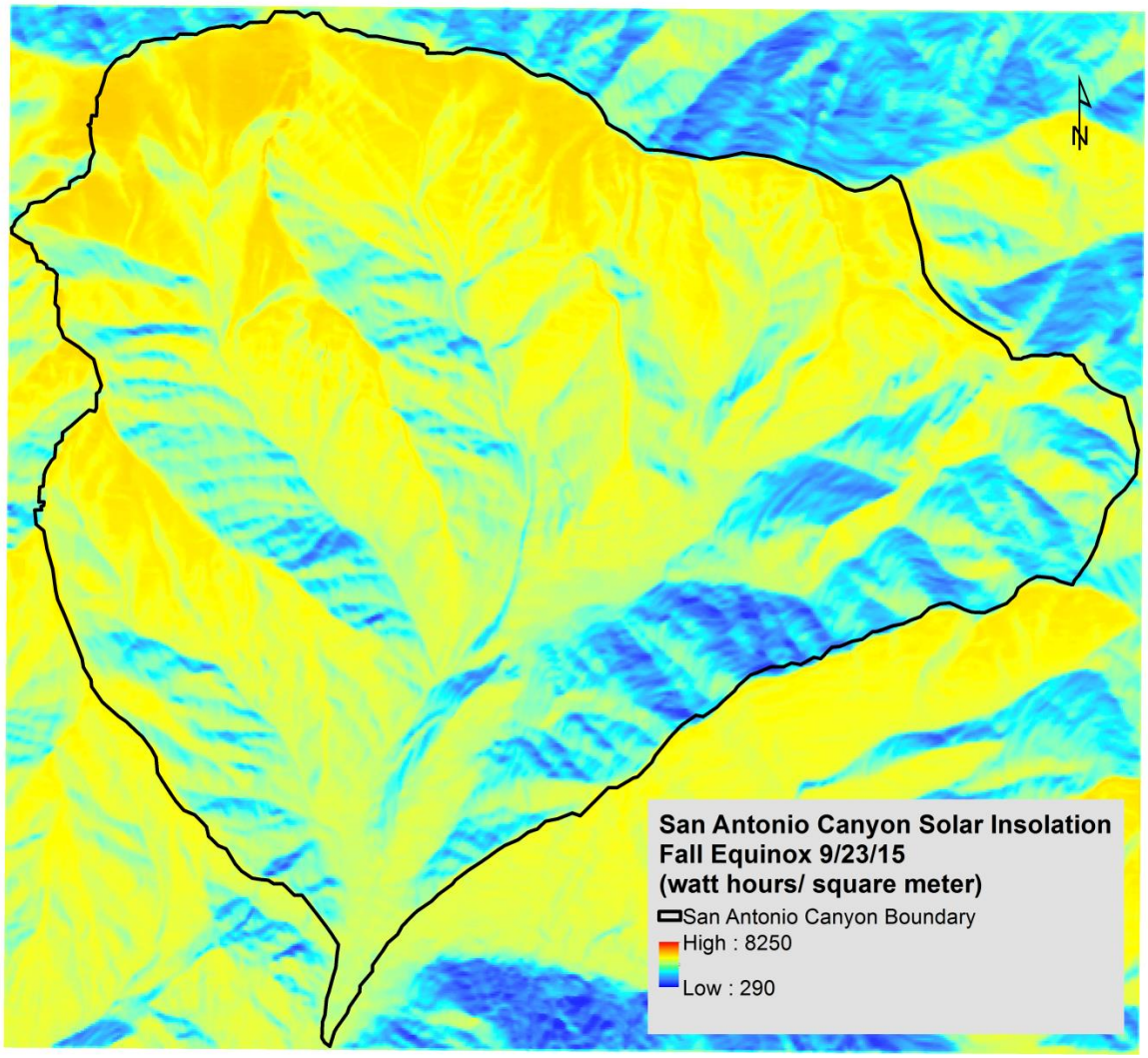

Figure 38. Solar insolation map for San Antonio Canyon-fall equinox.

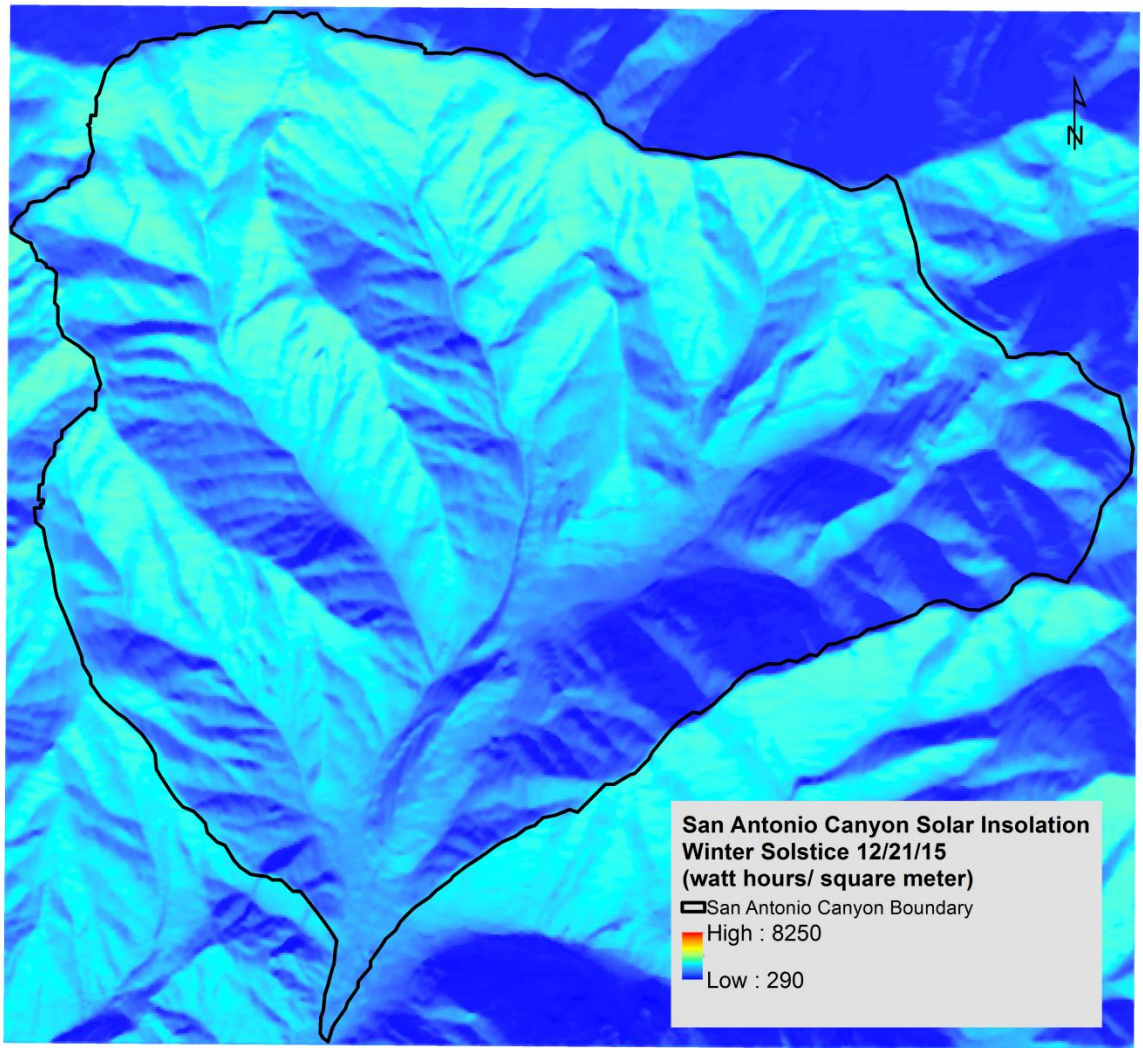

Figure 39. Solar insolation map for San Antonio Canyon-winter solstice.

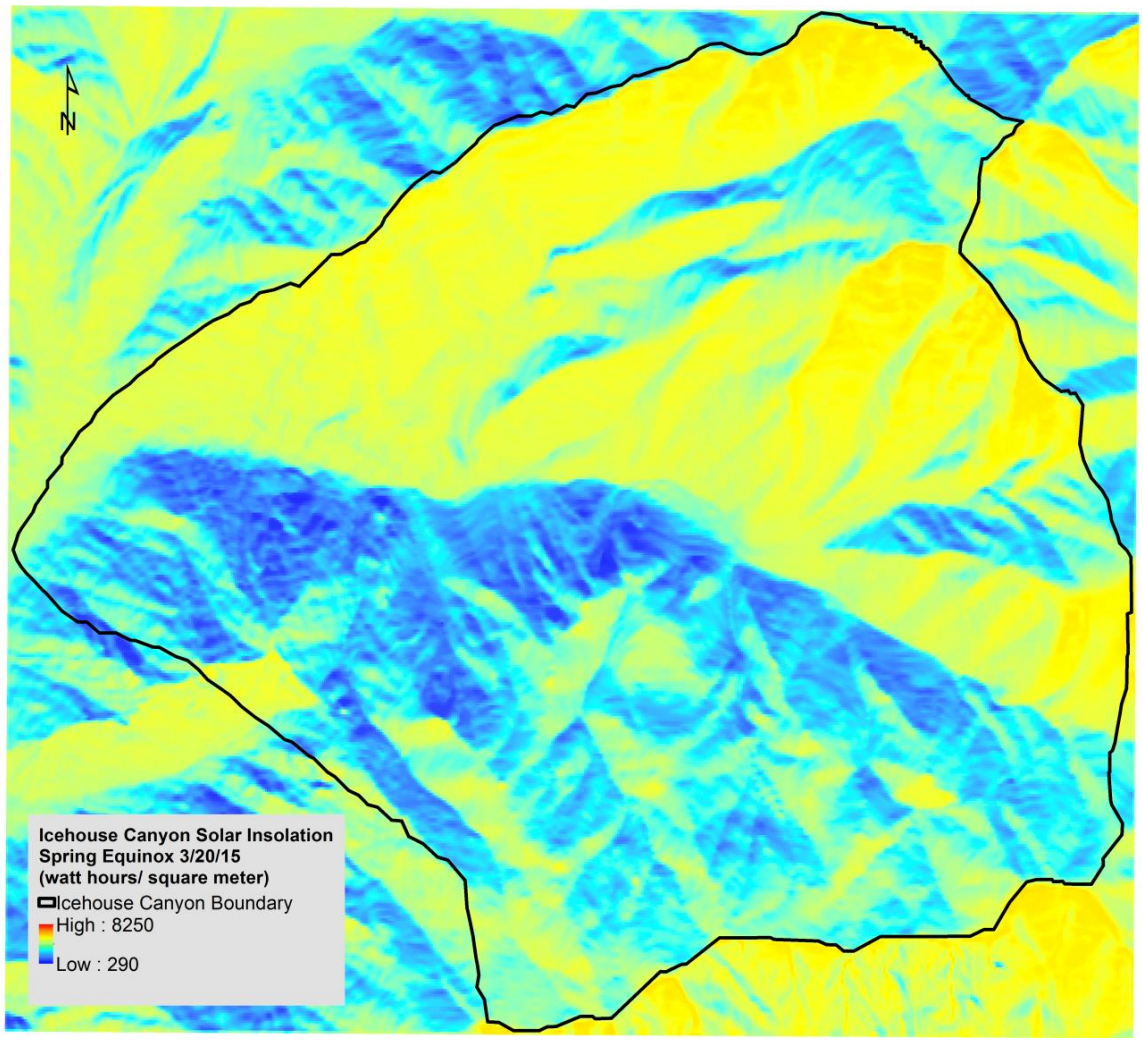

Figure 40. Solar insolation map for Icehouse Canyon-spring equinox.

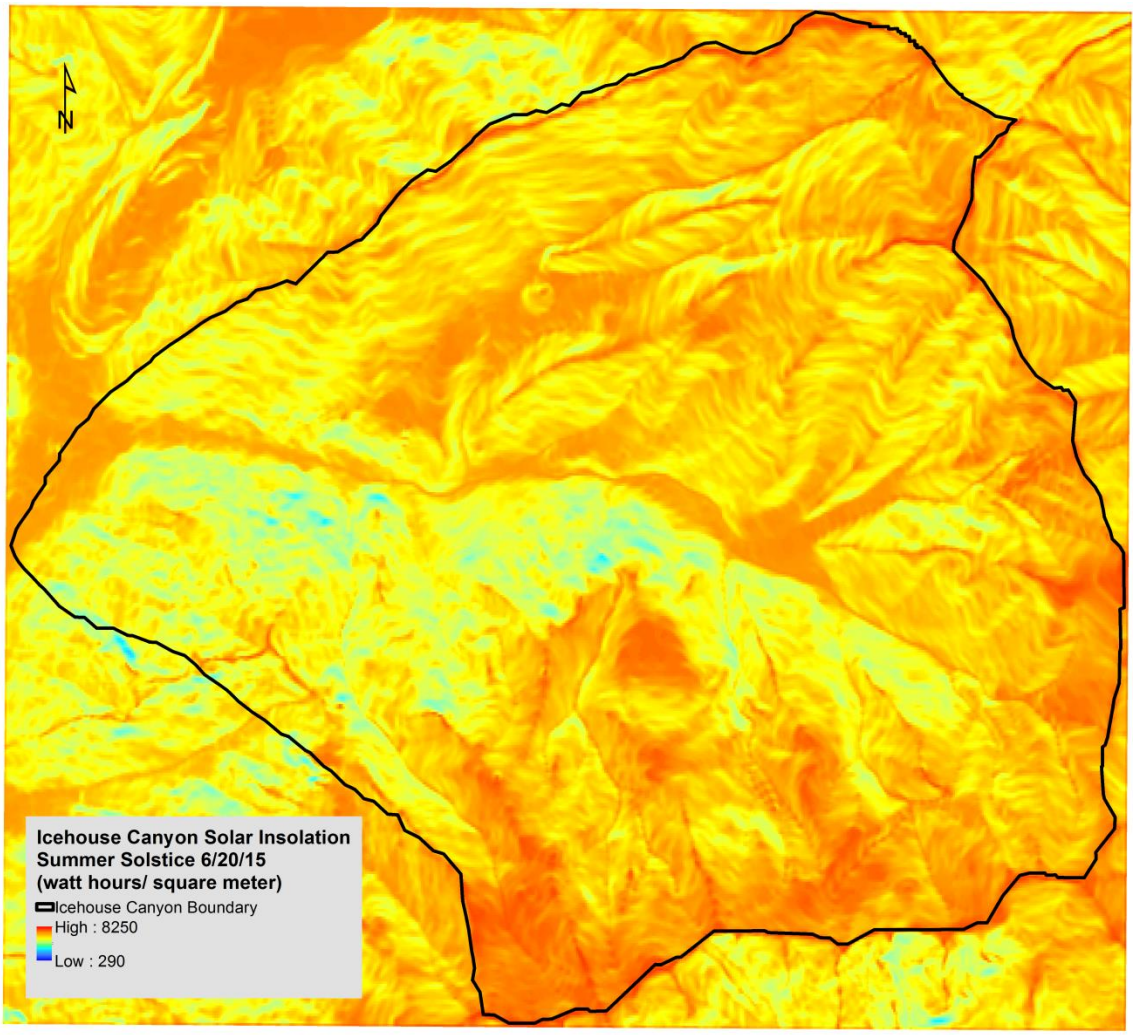

Figure 41. Solar insolation map for Icehouse Canyon-summer solstice.

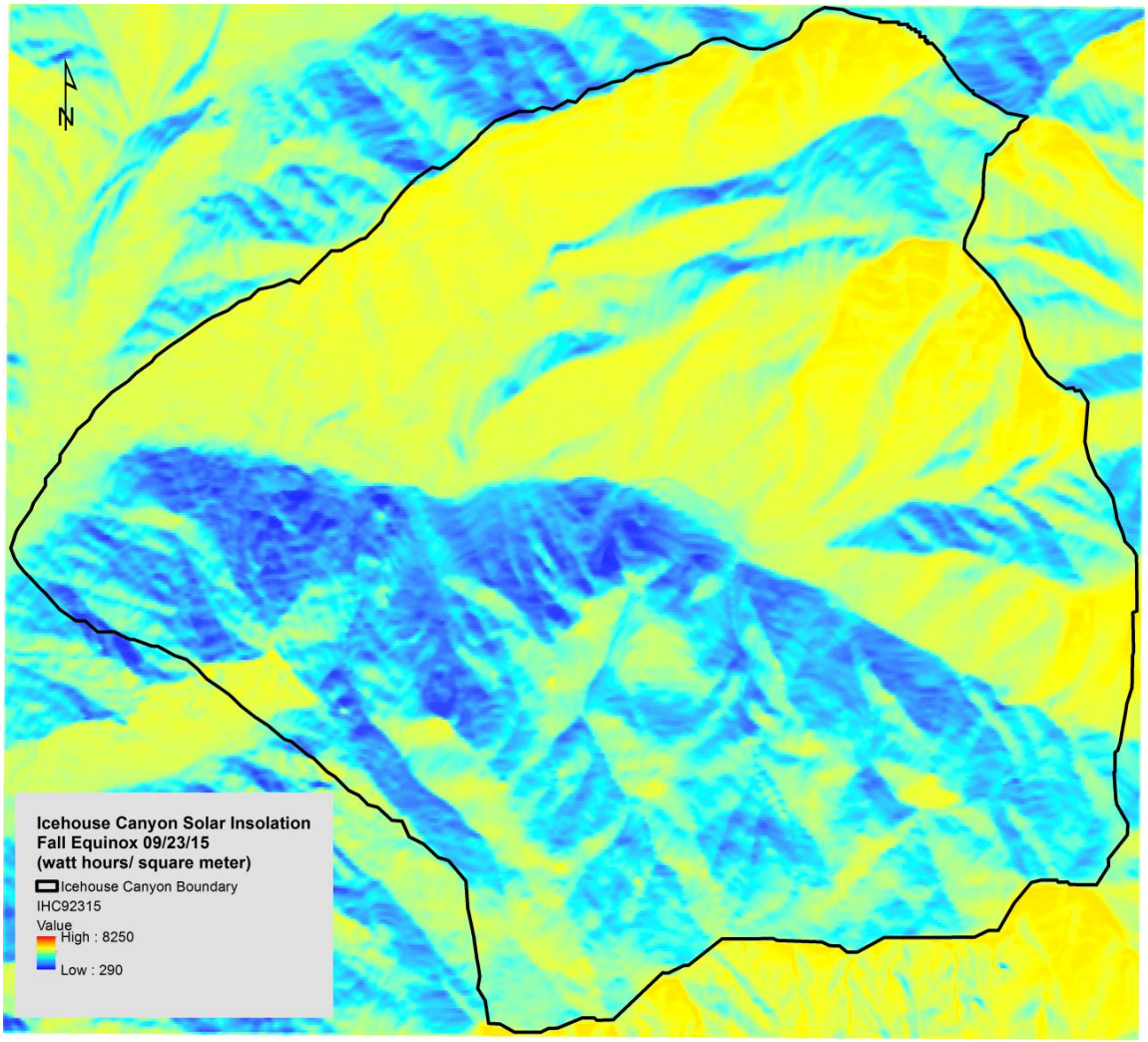

Figure 42. Solar insolation map for Icehouse Canyon-fall equinox.

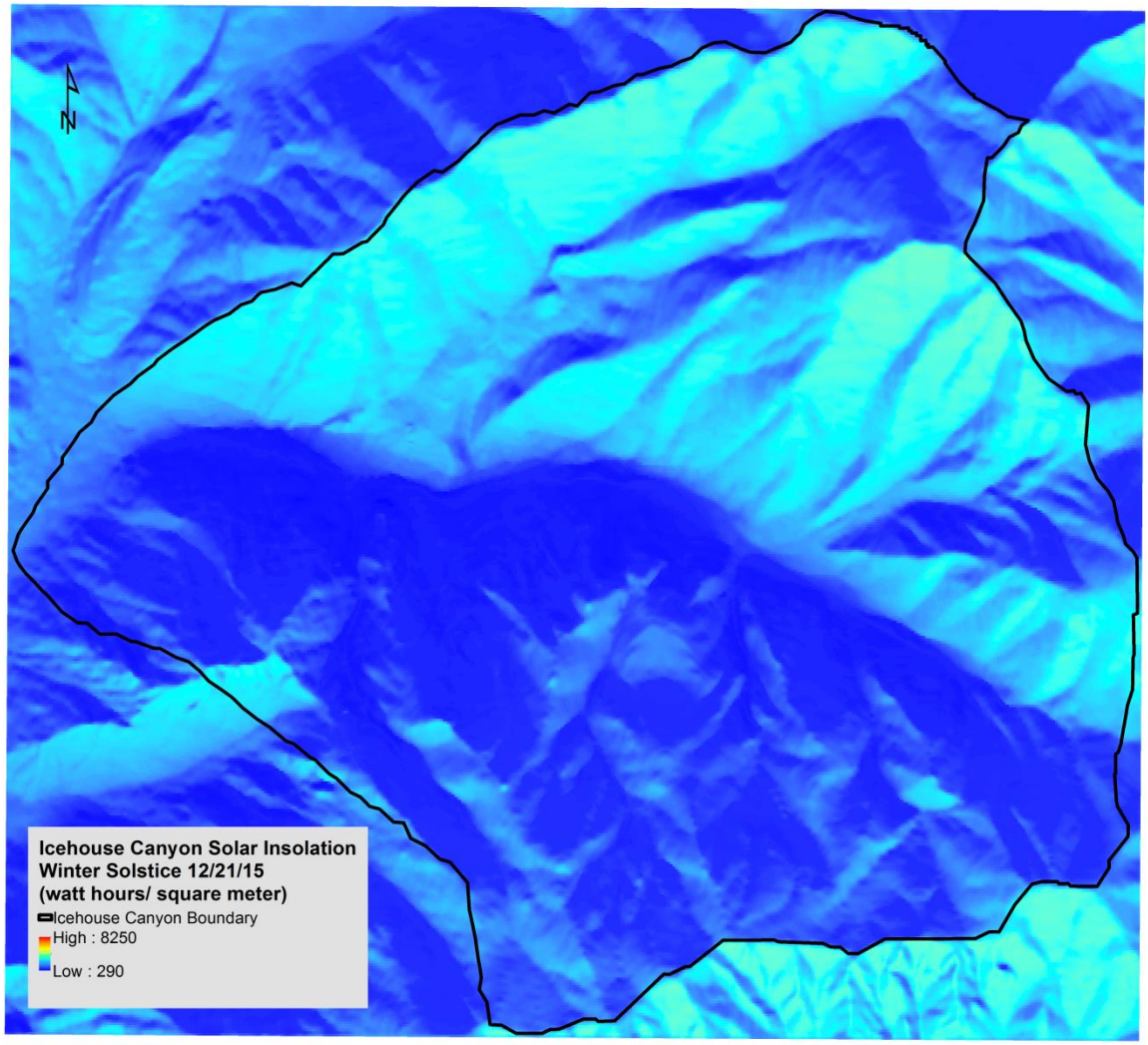

Figure 43. Solar insolation map for Icehouse Canyon-winter solstice.

CHAPTER 5

FIELD CHECKS AND CORRELATION OF IMAGERY

Field checks were performed to verify the vegetation present and some of the rock and soil units seen on the Google Earth™ imagery on various dates (1/26/14, 2/1/14, 6/23/14, 9/19/14, 12/28/14). Vegetation was noted as to the type and relative location in accessible areas throughout both watersheds. Vegetation was somewhat difficult to differentiate on the Google Earth™ imagery so it is extremely important to perform field checks in those areas that have ready access.

Field checks were also performed to observe the seasonal effects on vegetation. Some vegetation is evergreen and no change is observed between the imagery and the field; however, deciduous plants such as mountain mahogany (*Cerocarpus betulodes*) lose their leaves during the winter and look substantially different on the imagery. Locations of various plants, cultural objects, and rock/soil units were recorded using a Garmin® GPSmap78s unit to obtain GPS coordinates. These waypoints were then imported into the Google Earth™ maps to help understand the vegetation and rock/soil units present and correlated the interpretations made from the imagery to actual field data. Additional field GPS data was supplied from field work performed by Dr. Jon Nourse and Raymond Ng in July 2014 and gives control on the extent of the Cedar Canyon landslide located in Icehouse Canyon. A satellite image was printed out and notes on the various rock/soil unit and vegetation present were recorded directly on the image for use during digitization. These notes proved to be extremely useful for those areas that had no physical access. Vegetation and rock/soil inferences were able to be made for those inaccessible areas as a result of the field checks.

CHAPTER 6

INTERPRETATION AND DISCUSSION OF RESULTS

All of the maps created provide some measureable differences between the two watersheds whether it is the differences in the amount of shade, solar insolation, aspect, vegetation, rock/soil units, etc. Each of these maps contribute to the hypothesis that baseflow recession and evapotranspiration are controlled by a variety of interacting factors.

Correlation of Satellite Contacts with Conventional Mapping Contacts

Some correlations could not be made such as the correlation between bedrock exposure and anti-dip slopes in either of the two watersheds. Because the Google Earth™ image has an insufficient resolution, I was unable to correlate Nourse's unpublished strike and dip data with the bedrock exposures. Faulting did not seem to play a significant role that could be identified from the satellite imagery. Difficulties also arose in determining the actual contacts on the imagery. Again, resolution was the major problem. Conventionally mapped contacts with GPS coordinates will always be more accurate; however, traditional mapping does not have the benefit of being able to observe an entire area and are constrained to only those areas actually mapped. When DEM hill shade data was used to help locate contacts on the satellite image then the correlation between the satellite mapping and traditional mapping was very good.

For the covered bedrock, satellite mapping was again problematic. There were no clear indications between exposed bedrock and those areas with a veneer of soil. Most of the areas in both watersheds gradationally blend into one another. Some areas

within Icehouse Canyon however, showed enough differences between exposed bedrock and soil units so that it could be mapped as covered bedrock.

New Information Yielded by Satellite Mapping

In order to fully characterize each watershed, additional rock and soil units were needed as these can and most likely do affect the baseflow recession in the two canyons to some extent. Forest soils in mountainous regions tend to be thin; however, the forest is dependent upon these soils for moisture in addition to the underlying, weathered bedrock (Witty et al., 2003). The imagery upon detailed observation clearly shows that the soil and covered bedrock units are present. These units help to further refine the new Google Earth™ maps and are responsible in part for the differences seen in the calculated areas in Table 3 between the Dibblee and Nourse maps. Other differences in the maps are due to the subjective nature of mapping and the differences in how one identifies or defines the different rock units.

For the vegetation map, there is no existing detailed map of the two watersheds. The United States Department of Agriculture (USDA) Forest Service has geospatial data available for the general area that is based on automated, remote sensing, and photo editing with some limited field checking. The data has a minimum mapping size of 2.5 acres (10,117 sq. meters) for each vegetation class while I was able to look at individual plants as necessary. This resolution was especially useful in the riparian areas. My Google Earth™ vegetation map in general corresponded well regionally to the UDSA vegetation map.

Correlation of Vegetation with Rock and Soil Types

There are definite vegetation and rock/soil correlations that were observed in the watersheds. Vegetation types were used to help define rock/soil boundaries in both watersheds. It was noticed on the satellite image that chaparral was the predominant plant type found on the Cedar Canyon landslide. This was then used to help located the boundaries of several other landslides within Icehouse Canyon along with slope and hillshade information. However, chaparral was also found in other areas that contained loose, unconsolidated material such as talus so it cannot be used as the primary indicator for landslide deposits. Conifers were found throughout both canyons in the higher elevations on exposed bedrock because of their ability to extract water from deeper sources whereas oaks were only found in the lower elevations mostly below 2130 meters on north facing slopes.

Vegetation tends to be more dependent on the available water than the underlying rock or soil. Oaks are most commonly found in the canyon bottoms and those slopes that have a more mesic habitat, one that is more water balanced than the rest of the watersheds (Patric and Hanes, 1964). Both conifers and chaparral have deep root systems that will take advantage of existing available water especially during drought conditions and have the ability of penetrating down into fractured bedrock (Jones and Graham, 1993). Weathered bedrock is the interface between surficial soils and unweathered bedrock with a porosity that can store and transmit appreciable amounts of water (Sternberg et al., 1996). This zone can be many meters thick in places especially in those areas with shallow slopes and are free from mass wasting. Other areas have very thin mantles of soil where depth to bedrock can be less than 20

centimeters and the plants appear disproportionally large for the available soil (Jones and Graham, 1993).

Areas which have significant mass wasting will tend to have plants whose roots are able to penetrate deep down into the bedrock fractures. According to Hellmers,et al. (1955) fracturing and weathering are more marked in the metamorphic rocks than the harder granitic rocks in the San Gabriel Mountains both of which are present in the canyons. Vegetation plays a role in the amount of water in a soil by binding fine particles which in turn increases the residence time of water in a soil. Plants can affect the hydrology on a regional and local scale. At the local scale they increase the evapotranspiration and thereby decrease runoff; at the regional scale they give off water vapor. They also are able to influence soil permeability (Drever, 1993).

Map Variables and the Implications on Evaporation and Baseflow Recession

Important map variables were determined for the different iterations of the rock and soil maps that were digitized along with the DEM analyses to determine if there is support for hypothesis that the differences on the evapotranspiration and baseflow recessions seen in the two watersheds are partially a result of these variations. Aspect, slope angle, hill shade, and solar insolation variables were also determined. Carey (2009), Nourse (1994, 2010), and Vathanasin (1999) all speculated that these factors are present and contribute to the possible differences in evapotranspiration and baseflow recession; however, none had any quantitative data to support their hypotheses.

The three rock and soil maps all varied in the amounts of each unit present. The most likely reason for these differences is due to the emphasis placed on the mapped units by each mapper. Dibblee's map was primarily focused on the differing types of

crystalline bedrock present and hence his map has much more detail in the bedrock units as seen on the original maps used (Figure 9). Nourse's map focused on the more porous and permeable units, alluvium and talus, and their effects on groundwater in the watershed. My map is more of a conservative blend between the Nourse and Dibblee maps and is reflected in the values for each of the units (Table 3). Because of these differences, it can be assumed that the effects on the evapotranspiration and baseflow recessions for the watersheds will also be affected with more infiltration expected in areas of covered bedrock or soil which are more predominant in Icehouse Canyon based on the calculated areas or percentages. When the covered bedrock and soil amounts are taken into consideration for the two watersheds, the amounts of bedrock exposure between the Nourse map and my map become roughly equivalent.

Base flow recession is a measure of the time-dependent nature of discharge in a watershed during a dry period following precipitation recharge. The release of groundwater from porous rock or soil is an important factor in modulating the recession. High base flow recession constants (steep slopes on graphs of lnQ vs. time) indicate rapid drainage from the watershed after the rain stops. Such behavior might be expected in areas with abundant non-porous bedrock that would impede groundwater infiltration. Low base flow constants (shallow slopes on lnQ vs. time graphs) record more gradual, sustained drainage of groundwater into the trunk stream (or from a spring). This type of behavior might occur where thick soils absorb infiltrated precipitation during rain event, then release the water from the pores slowly over time by gravity drainage. A similar effect could be observed in areas of highly fractured bedrock, for example, near fault zones. Shallow slopes and flat areas have greater

capacity to absorb infiltrated precipitation, whereas steep slopes might display direct runoff in the form of overland flow during storm events.

Nourse's analysis on the baseflow recession rates are based in part on the measured surface discharge at multiple stream gages located along the Upper San Antonio Creek. He identifies two principle sources of groundwater found in the study area; infiltration into porous, permeable surficial deposits and infiltration into fractured and weathered bedrock. Figures 44-45 illustrate these sources (Nourse, 1994).

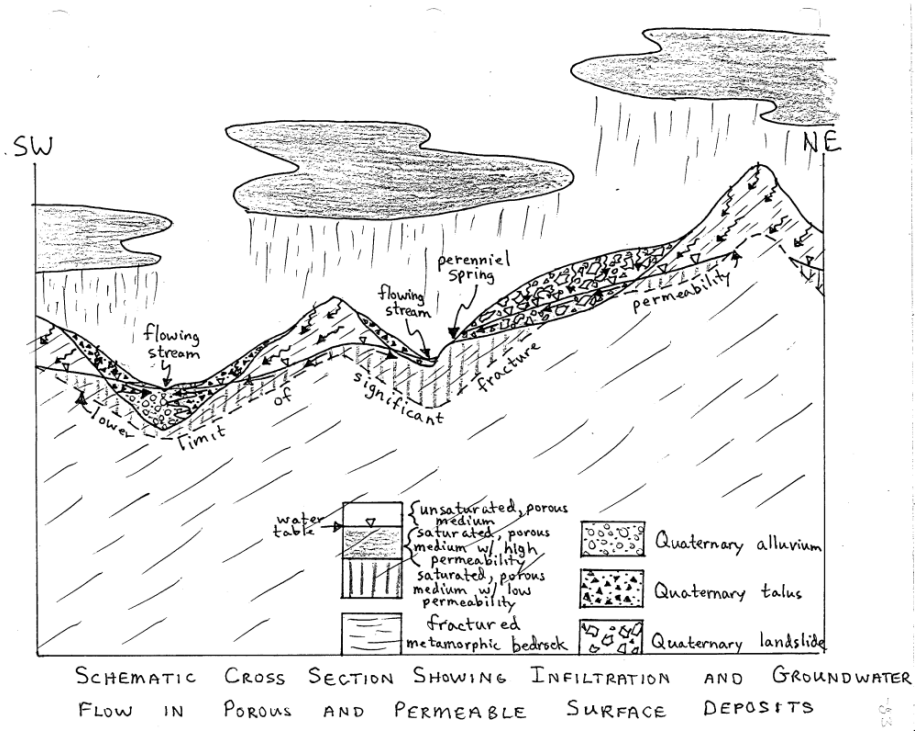

Figure 44. Schematic cross section showing infiltration and groundwater flow through surficial deposits. Reproduced courtesy of Dr. Jon Nourse (1994).

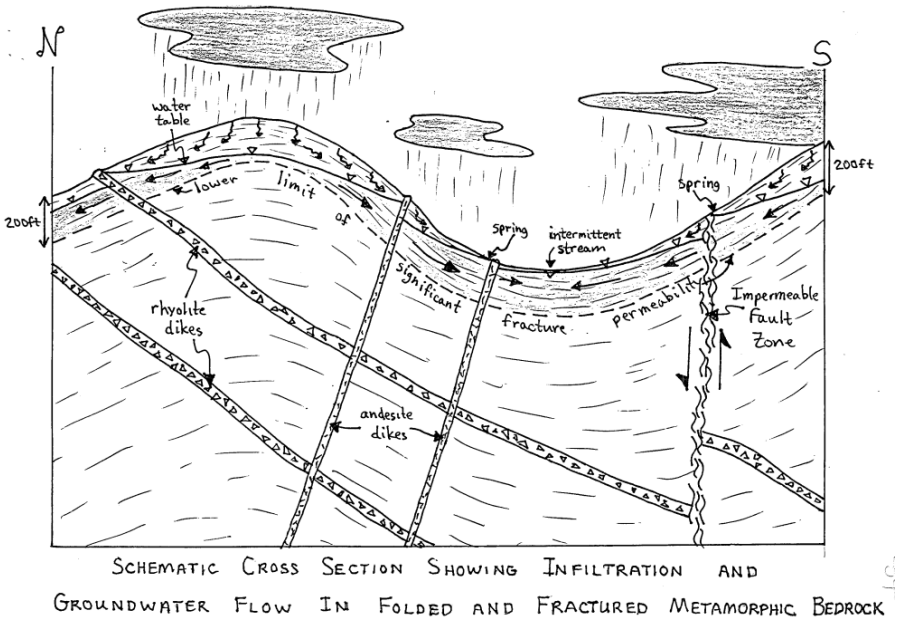

Figure 45. Schematic cross section showing infiltration and groundwater flow in bedrock. Reproduced courtesy of Dr. Jon Nourse (1994).

Given the baseflow recession rates (Table 1) for each watershed and the rock and soil maps it becomes clear which process predominates in Upper San Antonio Canyon and in Icehouse Canyon. San Antonio Canyon, with its extensive bedrock exposures, will tend to have less infiltration and have a higher discharge rate after precipitation events. Icehouse Canyon is the opposite with more landslides and covered bedrock units and hence it will have more infiltration into these surficial deposits with an expected lower discharge rate.

Vegetation again plays a role in evapotranspiration based on the other map variables of slope aspect, hill shade, and solar insolation. In Upper San Antonio Canyon the predominant vegetation type is the conifer and scrub unit which correlates well to the available groundwater pattern. Since the amount of precipitation that

retained in the watershed is less, it makes sense that the vegetation present must be able to tolerate a more drought-like condition than that of Icehouse Canyon.

Most of the slope faces (aspect) in San Antonio Canyon are oriented towards the south-southwest. As a result, the evapotranspiration rate should increase for those slopes faces that receive more direct solar insolation throughout the day. For Icehouse Canyon, there is a bimodal, north to south distribution of slope faces as seen in Figure 21. Icehouse Canyon would be expected to have a similar increase in evapotranspiration such as seen in San Antonio Canyon for the south facing slopes; however, for the north facing slopes, evapotranspiration would be expected to decrease since the amount of solar influx is much less as demonstrated in the solar insolation maps (Figures 40-43). Baseflow recessions constants should also be affected. The baseflow recession should increase for south facing slopes in both San Antonio and Icehouse Canyons while the north facing slopes in Icehouse Canyon should have a decrease in the baseflow recession constant due to less evapotranspiration taking place.

Slope angles play a role on evapotranspiration due to the quantity of water infiltrating into the watersheds. For steeply dipping slopes, it would be expected that there would be minimal infiltration and more runoff especially in those areas that have mostly crystalline bedrock present or thin mantles of soils. Those areas would suggest that there will be less evapotranspiration. In the areas with more gentle slopes, there are typically thicker soils present which would allow for more water retention and higher evaporation rates. Slope angles should also affect baseflow recessions constants by increasing the constant as slope angles increase.

Hill shade is significant primarily in Icehouse Canyon where the north facing slopes develop deep shade throughout the year. This will increase the amount of water available for vegetation and was seen in the distribution of moisture seeking oaks in canyon. Hill shade is not as significant in San Antonio canyon and would be expected to have only a minor impact on evapotranspiration and baseflow recession. For Icehouse Canyon, deep hill shade should increase the available water and decrease the baseflow recession constant.

Solar insolation is most likely the largest contributor to changes in evapotranspiration and baseflow recession constants than any of the other map variables studied since the sun is the driving force in the water cycle. San Antonio Canyon, as seen in Figures 36-39, shows that it receives more solar influx than does Icehouse Canyon. An evapotranspiration rate of 55% for San Antonio versus 47.6% Icehouse Canyon supports this hypothesis.

Hypsometric Data Analysis

Hypsometry is the measure of the relationship between elevation and a watershed's area (Strahler, 1952) and is a way to describe a watershed and the manner in which mass is distributed within the watershed (Figure 46). The hypsometric curve can be used to describe the maturity or evolution of the watershed. Curves that have a convex shape tend to be youthful watersheds while the more concave curves indicate an older watershed.

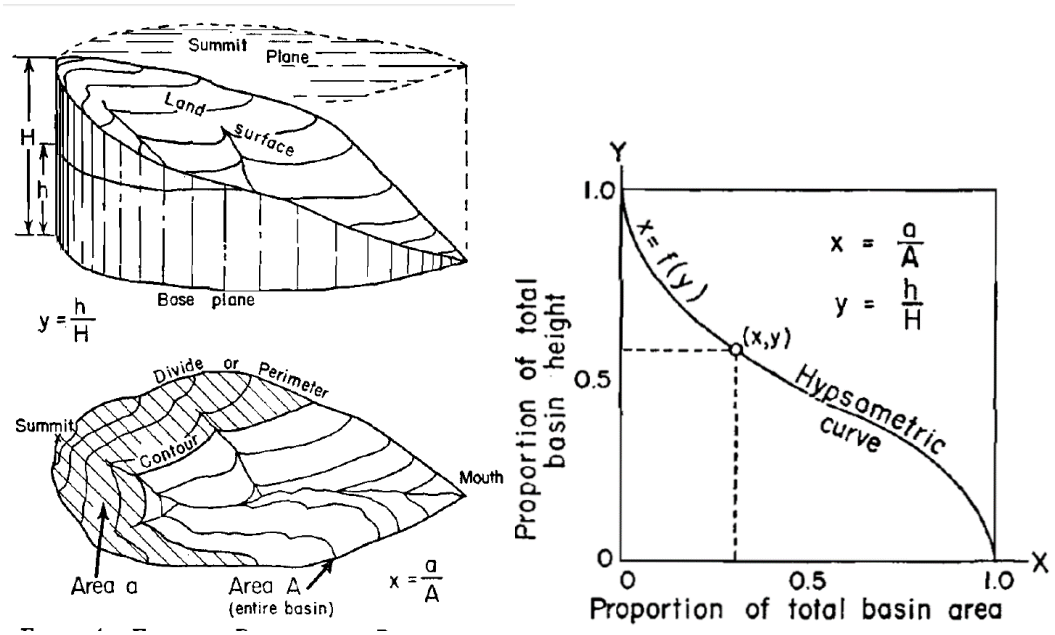

Figure 46. Reference basin with dimensionless parameters, (Strahler, 1952).

A hypsometric curve was developed for the two watersheds by using the same DEM used for the other map variables in the study. A special ArcMap geoprocessing hypsometric tool was obtained from ESRI that calculates the data needed to plot the hypsometric curve using Excel. The curves are shown in Figure 47.

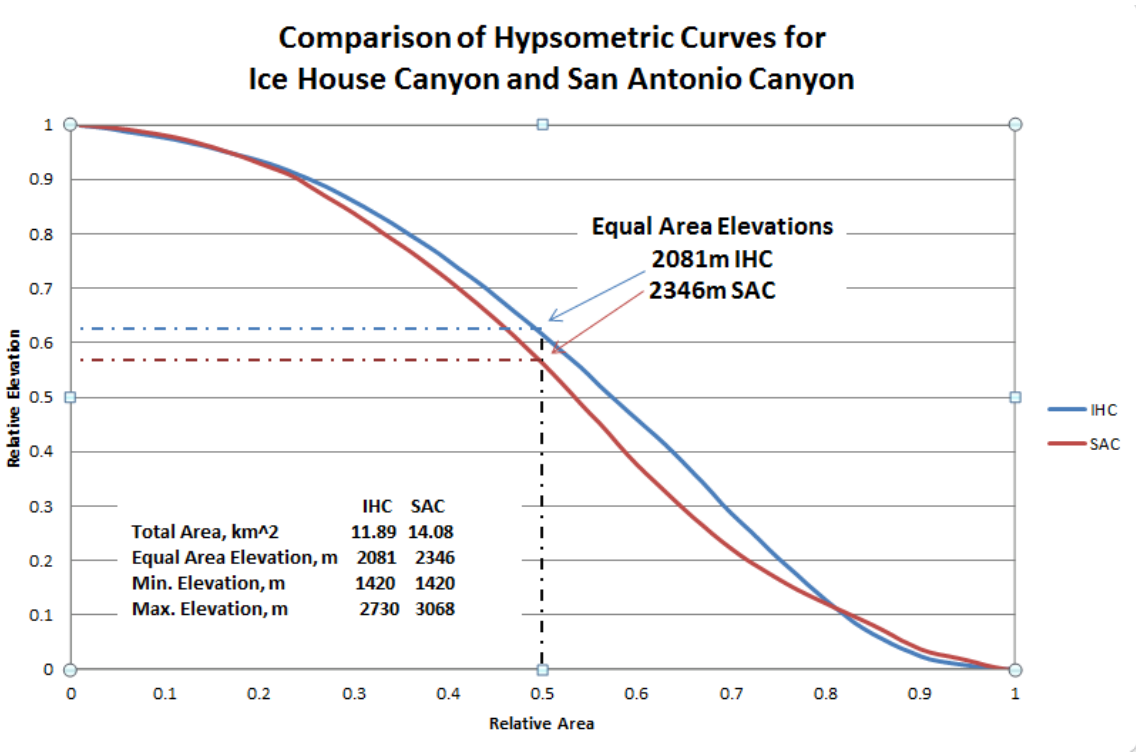

Figure 47. Hypsometric curves for San Antonio Canyon and Icehouse Canyon.

The resultant curves indicate that the two watersheds are similar in nature and hence they should have similar orographic trends. This would imply that the precipitation in the two watersheds are similar.

Comparison with Different Watersheds

Vathanasin's study (1999) of the San Dimas Experimental Forest (SDEF) hydrology and water budget provides data on the orographic precipitation within the two watersheds that he studied. He was able to relate this to the slope faces orientation where a measurable difference occurs between precipitation gages separated by less than two hundred feet and opposing each other in a north-south direction. This lends support to how my slope aspect data behaves in my two watersheds.

Vathanasin (1999) also calculated the evapotranspiration rate from vegetation to be 84% for his study area while Nourse (1996) calculated evapotranspiration to be 55%

and 47.6% for San Antonio Canyon and Icehouse Canyon respectively. Vegetation in the SDEF is denser than that of San Antonio and Icehouse canyons and the overall elevation is much lower in his study area. He also suggests that there are thicker deposits of soil in his study area and less exposed bedrock than in other nearby areas. These three factors can be attributed to the significant differences seen between the evapotranspiration rates of the two study areas.

Predictions for Other Watersheds

This study demonstrates that useful information can be derived using my method of mapping with Google Earth™ imagery and DEM data to identify rock, soil, and vegetation units especially for those inaccessible areas in the San Gabriel Mountains. My method can also be applied to other regions throughout southern California, such as the San Bernardino Mountains and the Sierra Nevadas, as the same type of vegetation exists in the region due to our unique Mediterranean-type climate.

Other areas that may benefit from a more detailed analysis are those areas in which water is already being impounded for domestic use. The water supply in California has decreased significantly over the past decade and warrants better management of this resource. Further work on the SDEF would be a good place to expand and refine this method of analysis since there are significant precipitation records available. Other local areas including the Big Tujunga and Cogswell dams may also benefit from more detailed analysis.

CHAPTER 7

CONCLUSIONS

This GIS analysis yields an important new data set that facilitates direct comparison of Icehouse Canyon and Upper San Antonio watersheds. The results illuminate spatial variations in geologic, biologic and solar parameters that influence observed differences in base flow recession and evapotranspiration. Below are the key conclusions:

- Significant differences can be seen in the types and amounts of vegetation present. Conifers were mostly seen in those areas that had a high percentage of bedrock exposure particularly at the higher elevations. Conifers have a deep root system that enables the plant the ability to obtain water from fractured bedrock sources. Oaks generally were seen on north facing slopes or in riparian zones bracketing nearby stream channels in Icehouse Canyon and San Antonio Canyon. Oaks were typically found in the lower elevations of the watersheds in areas where soil moisture is higher. Drought tolerant chaparral type vegetation was found on loose, unconsolidated material such as landslide or talus in both watersheds. Vegetation is more dependent on the available water present than the underlying bedrock or soil.
- Different rock and soil configurations exist between the two watersheds affecting baseflow recessions. San Antonio Canyon has more exposed bedrock present while Icehouse Canyon has significant amounts of covered bedrock present. Although all three iterations of the rock and soil maps had similar proportions of bedrock vs. alluvium vs. talus vs. landslide material, two

additional units of soil and covered bedrock were needed to better characterize the watersheds. These additional units have definite implications on the baseflow recessions averages seen for Upper San Antonio Canyon of 0.0185 $days^{-1}$ (Nourse, 2010) and 0.0081 $days^{-1}$ (Carey, 2009) for Icehouse Canyon.

- There are measurable differences in slope aspect. San Antonio Canyon has a predominant unimodal south-southwest face slope aspect while Icehouse Canyon has bimodal north and south facing slope aspects. This has implications for the amount of water present and retained in each canyon due to the amount of solar energy received throughout the year. Slopes that face south will receive more direct radiation than those that face north or east-west. Evaporation will be greatest for slopes facing south-southwest
- Slope angles are similar between the two canyons. Slope angles were determined and ranged from 0.20 to 75 degrees with the average slope of 34 degrees for both canyons.
- Hill shade and solar radiation are seasonally dependent. Hill shade and solar radiation maps showed distinct differences between the winter and summer solstices while the differences between the spring and fall equinoxes were measurable but negligible. All of these variables will have an effect on the overall water available for vegetation and thereby limiting certain types of vegetation to each canyon based on the microclimes present.
- The amount of solar radiation received is shown to be different for the two watersheds. Upper San Antonio Canyon receives more direct solar insolation

than does Icehouse Canyon regardless of season as seen in the histograms (Figure 35).

CHAPTER 8

RECOMMENDATIONS

Further research is needed in determining the actual boundaries of Cedar Canyon landslide. Work needs to be done in the future in areas that have fire damage. As these areas begin to regrow, vegetation types will change as the vegetation matures. After burns, the first plants to recover are those that can withstand fires and regenerate growth from the base of the plant as long as the roots remain unaffected. Several chaparral plants such as the laurel sumac have this capability. Vegetation secessions should be reassessed as these areas revegetate. Over time, chaparral should be replaced by oaks and conifers in the lower elevation areas while in higher elevations, mixed conifers would be the predominant vegetation.

Also, detailed gauging of springs and streams (using pressure transducers) as currently underway by graduate student Daniel Miranda would be helpful in refining the base-flow recession constants and real-time response to individual precipitation recharge events.

Additional field mapping recording GPS coordinates of covered bedrock and soil areas in Icehouse Canyon would I think be beneficial. Better control on the landslide deposits in Icehouse Canyon, specifically in the Ontario Peak and Bighorn Peak regions, would also help refine the baseflow recessions.

Solar insolation calculations of the actual amounts of radiation received would be extremely valuable but unfortunately quite complex. The solar insolation tool used only gives the amount of direct and diffuse radiation combined for each pixel or cell over a specified twenty four hour period but does not calculate the actual amounts of

radiation received for each watershed. Future work needs to be done on developing a way of calculating the amounts by using actual hours of sunlight and other variables such as the various solar angles and azimuths throughout the day, soil and rock reflectivity, topography angle (slope), atmospheric adsorption of radiation, etc.

Another variable that should be investigated is how snow affects evapotranspiration and baseflow recession constants for the canyons. Does snow melt make any significant contribution to the baseflow constant determined for San Antonio and Icehouse Canyons?

REFERENCES

Bond, B. J., Jones, J. A., Moore, G., Phillips, N., Post, D., and McDonnell, J. J., 2002, the zone of vegetation influence on baseflow revealed by diel patterns of streamflow and vegetation water use in a headwater basin: Hydrological Processes, v. 16, p. 1671-1677.

Bosch, J. M., and Hewlett, J. D., 1982, A review of catchment experiments to determine the effect of vegetation changes on water yield and evapotranspiration: Journal of Hydrology, v. 55, p. 3-28.

Brown, A. E., Zhang, L., McMahon, T. A., Western, A. W., Vertessy, R. A., 2005, A review of paired catchment studies for determining changes in water yield resulting from alterations in vegetation: Journal of Hydrology, v. 310, p. 28-61.

Carey, L. R., 2009, Analysis of baseflow recession in Icehouse Canyon, San Gabriel Mountains, CA, [senior thesis]: Pomona, California State Polytechnic University.

Davis, J., 2010, Hypsometric Tool: A geospatial tool for deriving hypsometry (area/elevation) for a watershed elevation raster: ESRI ArcScripts Support.

Dibblee Jr., T. W., 2002, Geological map of the Mount San Antonio quadrangle, scale 1:24 000, 1 sheet.

Dibblee Jr., T. W., 2002, Geological map of the Mount Baldy quadrangle, scale 1:24 000, 1 sheet.

Dibblee Jr., T. W., 2003, Geological map of the Cucamonga Peak quadrangle, scale 1:24 000, 1 sheet.

Dibblee Jr., T. W., 2003, Geological map of the Telegraph Peak and Phelan quadrangle, scale 1:24 000, 1 sheet.

Dole, J. W., and Rose, B.B., 1996, Shrubs and trees of the southern California chaparral and mountains, an amateur botanist's identification manual, Footloose Press, California.

Drever, J. I., 1994, The effect of land plants on weathering rates of silicate minerals: Geochimica et Cosmochimica Acta, v. 58, no. 10, p. 2325-2332.

Farmer, D., Sivapalan, M., and Jothityangkoon, C., 2003, Climate, soil, and vegetation controls upon the variability of water balance in temperate and semiarid landscapes: downward approach to water balance analysis: Water Resources Research, v. 39, no. 2, 1035, doi:10.1029/2001WR000328, 2.

Flerchinger, G. N., Hanson, C. L., Wight, J. R., 1996, Modeling evapotranspiration and surface energy budgets across a watershed: Water Resources Research, v. 32, no. 8, p. 2539-2548.

Fu, P., and Rich, P. M., 1999, Design and implementation of the solar analyst: an ArcView extension for modeling solar radiation at landscape scales, *in* Proceedings, ESRI Users Conference, p867.

Hanes, T. L., Friesen, R. D., and Keane, K., 1989, Alluvial scrub vegetation in coastal southern California, *presented* at California Riparian Systems Conference, Sept. 22-24, 1988, USDA Forest Service Technical Report, PSW-110.

Harder, C., Ormsby, T., and Balstom, T., 2013, Understanding GIS: an ArcGIS project workbook: 2ed., ESRI press, Redlands, CA.

Hellmers, H., Horton, G., Juhren, G., O'Keefe, J., 1955, Root systems of some chaparral plants in Southern California: Ecology, v. 36, no. 4, p. 667-678.
Hewlett, J. D., 1961, Soil moisture as a source of base flow from steep mountain watersheds: Southeast Forest Experiment Station, Asheville, North Carolina, US Dept. of Agriculture-Forest Service, station paper no. 132.
Hibbert, A. R., 1968, Forest treatment effects on water yield: Coweeta Hydrologic Laboratory, Southeast Forest Experiment Station, Asheville, North Carolina, US Dept. of Agriculture, p. 527-543.
Hubbert, K. R., Beyers, J. L., and Graham, R. C., 2001, Roles of weathered bedrock and soil in seasonal water relations *Pinus Jeffreyi* and *Arctostaphylos patula*: Canadian Journal of Forest Resources, v. 31, p. 1947-1957.
Huxman, T. E., Wilcox, B. P., Breshears, D. D., Scott, R. L., Snyder, K. A., Small, E. E., Jultine, K., Pockman, W. T., and Jackson, R. B., 2005, Ecohydrological implications of woody plant encroachment: Ecology, v. 86, no. 2, p. 308-319.
Jones, D. P., and Graham, R. C., 1993, Water holding characteristics of weathered granitic rock in chaparral and forest ecosystems: Soil Science Society of America, v.57, p. 256-261.
Law, M., and Collins, A., 2013, Getting to know ArcGIS for desktop: 3ed., ESRI press, Redlands, CA.
Maher, M. M., 2010, Lining up data in ArcGIS, 2ed., ESRI press, Redlands, CA.
Nourse, J. A., unpublished mapping, 1991-2003.
Nourse, J. A., 1994, Water resources of upper San Antonio Creek watershed, eastern San Gabriel Mountains, California, report submitted to Snowcrest Heights Improvement Association, Mt. Baldy, California, one plate and 86 p.
Nourse, J. A., Carey, L. R., Bautz, M., and Reily, J., 2010, Hydrogeology of Icehouse Canyon, contrasted with Upper San Antonio watershed, San Gabriel Mountains, California, *in* Clifton, H. E. and Ingersoll, R. V., eds., Geologic excursions in California and Nevada: tectonics, stratigraphy and hydrogeology: Pacific Section, Society for Sedimentary Geology, Guidebook 8, p. 323-347.
Nourse, J. A., and Vathanasin, V. A., 1996, Geobotanical reasons for contrasting water budgets in two ocean-facing drainage basins, San Gabriel Mountains, California, Geological Society of America Abstracts with Programs, v. 31, no. 7, p. 413-414.
Patric, J. H., and Hayes, T. L., 1964, Chaparral succession in a San Gabriel Mountain area of California: Ecology, v. 45, no. 2, p. 353-360.
Price, K., 2011, Effects of watershed topography, soils, land use, and climate on baseflow hydrology in humid regions: a review: Progress in Physical Geography, v. 35, no. 4, p. 465-492.
Quinn, R. D., and Keeley, S. C., 2006, Introduction to California chaparral: University of California Press.
Rundel, P. W., and Gustafson, R., 2005, Introduction to plant life of southern California, coast to foothills: University of California Press.
Rodriguez-Iturbe, I., 2000, Ecohydrology: a hydrologic perspective of climate-soil-vegetation dynamics: Water Resources Research, v. 36, no. 1, p. 3-9.
Sternberg, P. D., Anderson, M. A., Graham, R. C., Beyers, J. L., and Tice, K. R., 1996, Root distribution and seasonal water status in weathered granitic bedrock under chaparral: Geoderma, v. 72, p. 89-98.

Stevenson, N. L., 1998, Actual evapotranspiration and deficit: biologically meaningful correlates of vegetation distribution across spatial scales: Journal of Biogeography, v. 25, p. 855-870.
Strahler, A.N., 1952, Hypsometric (Area-Altitude) analysis of erosional topography: Bulletin of the Geological Society of America, v.63, p. 1117-1142.
Strand, J., 2006, Impact of wildfires on historical and modern analysis of baseflow recession in the San Dimas watershed, [senior thesis]: Pomona, California State Polytechnic University.
Tallaksen, L. M., 1995, A review of baseflow recession analysis: Journal of Hydrology, v. 165, p. 349-370.
Vathanasin, V., 1999, Hydrology and water budget of the San Dimas Experimental Forrest, San Gabriel Mountains, California, [senior thesis]: Pomona, California State Polytechnic University.
Wittenberg, H., and Sivapalan, M., 1999, Watershed groundwater balance estimation using streamflow recession analysis and baseflow separations: Journal of Hydrology, v. 219, p. 20-33.
Witty, J. H., Graham, R. C., Hubbert, K. R., Doolittle, J. A., and Wald, J. A., 2003, Contributions of water supply from the weathered bedrock zone to forest soil quality: Geoderma, v. 114, p. 389-400.
Zecharia, Y. B., and Brutsaert, W., 1988, Recession characteristics of groundwater outflow and base flow from mountainous watersheds: Water Resources Research, v. 24, no. 10, p. 1651-1658.
Zhang, L., Dawes, W. R., and Walker, G. R., 2001, Response of mean annual evapotranspiration to vegetation changes at catchment scales: Water Resources Research, v. 37, no. 3, p. 701-708.
Zwieniecki, M. A., and Newton, M., 1995, Roots growing in rock fissures: their morphological adaptation: Plant and Soil, v. 172, p. 181-187.
www.willcogis.org/imf/ext/geocortex/compass/gcx_tut1 (January 2015)
http://webhelp.esri.com/arcgisserver/9.3/java/index.htm#geodatabases/topology_basics (January 2015)